Nonlinear Processes in Geophysics (1999) 6: 99–127

Nonlinear Processes in Geophysics

Comments and new results about the magnetospheric chaos hypothesis

G. P. Pavlos, M. A. Athanasiu, D. Diamantidis, A. G. Rigas and E. T. Sarris

Department of Electrical and Computer Engineering, Demokritos University of Thrace, 67 100 Xanthi, Greece

Received: 09 January 1999 – Accepted: 17 April 1999

Abstract. In this study we present theoretical concepts and results concerning the hypothesis test of the magnetospheric chaos. For this reason we compare the observational behavior of the magnetospheric system with results obtained by analyzing different types of stochastic and deterministic input-output systems. The results of this comparison indicate that the hypothesis of low-dimensional chaos for the magnetospheric dynamics remains a possible and fruitful concept which must be developed further.

1. Introduction

Ten years ago we used the concept of strange attractor dynamics as explicative paradigm of magnetospheric substorms (see Pavlos, 1988). By this it is implied that the magnetospheric substorms can be explained as the effect of nonlinear dynamics of the magnetospheric physical state on a strange attracting subset of the (phase-space) corresponding to the magnetospheric dynamics. Baker et al. (1990) have studied the solar-wind magnetosphere coupling problem using a nonlinear dripping faucet analogy of the system. This approach was motivated by the laboratory study of the dripping faucet (Shaw, 1984) and also by the dripping faucet description of plasmoid formation and release discussed by Hones (1979). Baker's model of the magnetospheric dynamics is a mechanical analog. Klimas et al. (1991, 1992) developed the Faraday loop response model. Pavlos et al. (1994) extended the linear magnetospheric equivalent electric circuit of Liu et al. (1988) to a nonlinear one. The nonlinear modeling of magnetospheric dynamics has given results supporting the concept of magnetospheric chaos (see also Vassiliadis et al., 1990; Shan et al., 1991; Roberts et al., 1991; Prichard and Price, 1992; Pavlos et al., 1992a, b; Vassiliadis et al., 1992; Sharma et al., 1993 and Takalo and Timonen, 1994).

Parallel to these studies a fruitful criticism has been developed about the supposition of magnetospheric chaos especially in relation to its experimental evidence. Prichard and Price (1992, 1993) showed that many of the previous results supporting the concept of low-dimensional magnetospheric dynamics were caused by the long decocorrelation time of the AE index and therefore were not the result of low-dimensional dynamics. Osborne and Provenzale (1989), Provenzale et al. (1992), Theiler (1991), Pavlos et al. (1992a, b) used many tests in order to exclude the pseudo-chaos of colored noises. The term pseudo-chaos was introduced by Pavlos et al. (1992a,b) to discriminate the real low-dimensional chaotic dynamics contained in aperiodic time series from stochastic time series (nonchaotic and aperiodic time series) which can mimic almost indistinguishably the phenomenology of chaotic time series. Moreover, Vassiliadis et al. (1992) used the Theiler's test in the case of magnetospheric data and showed that, when the parameter w of Theiler becomes comparable to the decocorrelation time, the scaling in the correlation integral disappears and there was no convergence of its slopes. Pavlos et al. (1994) extended the chaotic analysis to the AE index by using singular value decomposition (SVD) analysis according to Broomhead and King (1986). Sharma et al. (1993) had also used SVD analysis for the estimation of the eigenvalue spectrum of the AE index. The combination of SVD analysis and the Theiler test in the work of Pavlos et al. (1994) has given strong evidence for the existence of magnetospheric chaos especially when the Theiler's parameter w is equal to the decorrelation time. Prichard (1995) in a short comment strongly criticize the results presented in the work of Pavlos et al. (1994). In their criticism they use the method of surrogate data and the method of Takens (1985) for the estimation of correlation dimension. Their conclusion was that there is no evidence

Correspondence to: G. Pavlos

that the AE index can be described by a low-dimensional strange attractor. An extended review of studies of nonlinear dynamics of the magnetosphere is given by Klimas et al. (1996). Our intention in a series of papers is to present a possible answer to the criticism about the magnetospheric chaos. In two studies (Pavlos et al., 1999a, b) we show that the detailed statistical comparison of geometrical and dynamical magnitudes corresponding to the AE index time series and its nonlinear surrogate data (Theiler et al., 1992a,b) reveal significant differences. These results indicate strongly the non-linearity and low dimensionality of the AE index. Here we extend our previous work aiming at confronting further the dilemma about the hypothesis of magnetospheric chaos. In section *2* we summarize the crucial points of the above criticism. In sections *3*, *4* and *5* we introduce significant theoretical concepts about the magnetospheric system and its dynamical interaction with the solar wind. In section *5* we describe important aspects of classical and modern time series analysis as well as aspects of stochastic systems and input-output dynamical systems related to the magnetospheric dynamics. In section *6* we present new results concerning stochastic dynamics and input-output dynamics by using appropriate systems which in a way can mimic the magnetospheric system. In section *7* we present results by applying the nonlinear time series analysis on two new magnetospheric time series. Finally in section *8* we summarize the theoretical concepts and the experimental results for a comparison and better understanding of the magnetospheric dynamics.

2. A brief description of the criticism against magnetospheric chaos

The criticism of Prichard (1995) is based on the method of surrogate data. According to this method the geometrical or dynamical characteristics of an experimental time series must be compared with stochastic signals which have the same power spectrum and amplitude distribution as the original data. If the difference is not significant then we are unable to conclude chaotic behavior in the experimental data (Theiler et al., 1992a,b). Prichard (1995) have used this method for the correlation dimension of the AE index and they assert that:

a) The correlation dimension of AE index time series cannot be distinguished from that of a stochastic signal with the same power spectrum and amplitude distribution as the original data.
b) There is no evidence for the existence of low-dimensionality according to their estimate of correlation dimension obtained by using Takens' method.
c) There is some evidence for nonlinearity in the AE index time series. It is not clear whether the nonlinearity of the AE index is the result of the intrinsic dynamics of the magnetosphere or the result of the nonlinearity in the solar wind.
d) Because the magnetosphere is largely controlled by the solar wind this alone should provide evidence against the existence of a strange attractor in the AE index as the magnetosphere is a randomly driven non-autonomous system.
e) There is no evidence for low dimensionality of the AE index and no evidence that the AE index can be described by a low dimensional strange attractor.

In two previous studies by Price and Prichard (1993) and Price et al. (1994) we can also notice contradicting results concerning the coupling of the magnetosphere with the solar wind. Firstly, Price and Prichard (1993) by using non-linear statistics and non-linear prediction of the response to the input signals of the solar wind conclude some evidence for deterministic non-linear responce of the Earth's magnetosphere. Secondly Price et al. (1994) by using also nonlinear input-output analysis in the form of a prediction scheme and for different combinations of the solar wind variables as input functions they conclude that in no case the evidence for nonlinear coupling between the input and the output is particularly strong. Moreover we must notice two different declarations in the criticism by Prichard (1995). In the first they declare that "... *the original data cannot be distinguished from the surrogate data sets using the Takens estimator* ..." and in the second a few lines later they write "...*it is clear that the original data can be distinguished from the surrogates, so there is some evidence for nonlinearity* ...". Therefore we notice a kind of theoretical and observational obscurity in the existent criticism about the internal dynamics of the magnetospheric system, as well as about its external coupling. This is obvious especially when the driven and non autonomous character of the magnetosphere is taken as evidence against the hypothesis of magnetospheric chaos as it was summarized previously (see point d). However the last remarks cannot reduce at all the fertility of the criticism about the magnetospheric chaos hypothesis by the above scientists. In contrast the existed criticism presses for a deeper theoretical and experimental study of the magnetospheric system. For this we look at the question spherically in the following by examining the theoretical and experimental characteristics of the magnetospheric dynamics especially from the point of view of an externally driven system.

3. Modeling the magnetospheric dynamics and the magnetospheric randomness.

The earth's magnetospheric system is caused by continuous and self-consistent electromagnetic interaction of the earth magnetic field and the solar wind plasma. The result of this interaction is the earth's magnetosphere, a complex system with many internal subsystems and processes. In

this system the magnetotail plasma sheet is of central importance. Other importance subsystems are the lobes, the plasma sphere, the plasma mantle, the higher ionosphere, the boundary layers and the magnetopause (Kan, 1991). Either as a plasma system or as an electric current system the magnetospheric system is strongly non-linear and dissipative. That is the Maxwell-Vlasov equations and their macroscopic magnetohydrodynamical (MHD) expression taken for the magnetospheric system correspond to a non-linear and dissipative plasma system. In a collisionless plasma, as it is the magnetospheric plasma, microturbulent electric and magnetic fields excited by plasma instabilities produce irregular transport coefficients such as resistivity, viscocity, diffusion and heat conduction, (Papadopoulos, 1980). These irregular transport coefficients can introduce strong nonlinearity and dissipativity in the internal magnetospheric processes. On the other hand we know that nonlinearity and dissipativity are two necessary conditions for the existence of chaotic dynamics (Argyris et al., 1994; Tsonis, 1992).

The first natural paradigm of chaotic dynamics was the study of the flow in fluids (Lorenz, 1963) by the Navier-Stokes equations, which includes the temperature and the velocity fields, as well as the density and the fluid pressure fields as the crucial physical magnitudes. Lorenz used appropriate boundary conditions and retained only the lowest order forms in Fourier expansion of fields to get the famous Lorenz 3-dimensional dynamical system. The solution of the Lorenz system bifurcates gradually from stable (limit point) to periodic (limit cycle) and chaotic attractors as we increase the values of its control parameters. The above paradigm of chaotic behavior permits us to suppose that chaos can be a possible hypothesis for a bounded magnetized fluid as happens with the magnetospheric plasma system. For space plasmas the Navier-Stokes equations will need to be altered in order to take into account, besides gravity, the electrodynamic force $\boldsymbol{F}=\rho\boldsymbol{E}+\rho\boldsymbol{v}\boldsymbol{x}\boldsymbol{B}$ exercised on the charges. Maxwell's equations will have also to be considered in order to get a closed system of equations. The generalization of Navier-Stokes equations besides the mechanical variables must also include variables connected to the electromagnetic field $\{\boldsymbol{E}(\boldsymbol{x}, t), \boldsymbol{B}(\boldsymbol{x}, t)\}$. After this similarity with the Lorenz system chaotic solutions for magnetized and electrically conducting fluids or magnetized plasmas have been found too (Bhattacharjee, 1987; Weiss et al., 1984; Spiegel and Weiss, 1980; Weiss, 1990; Spiegel, 1985; Summers and Mu, 1992). An active area of dynamical systems is devoted to proving the existence of finite dimensional attractors in various partial differential equations (Haken, 1983 ; Tsonis, 1992; Argyris et al., 1994) The central manifold theory is a candidate theory for explaining the reduction of dimensionality in an infinite or finite dimensional system. This theory permits to describe different kinds of macroscopic spatio-temporal patterns in a system with infinite degrees of freedom as happens with space plasmas in the magnetosphere, solar wind or the convective zones of stars like the Sun. Although, for the magnetospheric system we have not a developed form of the central manifold theory, in the following we present some crucial points as a general support of the magnetospheric chaos hypothesis. A magnetized plasma system (described as a fluid) has infinite degrees of freedom consisted of physical (observable) variables as temperature, density, velocity, pressure, electric and magnetic fields, defined at every point x of the space. All these variables constitute the physical state $\boldsymbol{U}(\boldsymbol{x},t)$ given by

$$\boldsymbol{U}(\boldsymbol{x},t)=\{\boldsymbol{V}(\boldsymbol{x},t),P(\boldsymbol{x},t),n(\boldsymbol{x},t),T(\boldsymbol{x},t),\boldsymbol{E}(\boldsymbol{x},t),\boldsymbol{B}(\boldsymbol{x},t)\ldots\} \tag{3.1}$$

which evolves through an infinite dimensional phase space.

The temporal evolution of this plasma system is described by nonlinear partial differential equations of the general form

$$\partial_t \boldsymbol{U}(\boldsymbol{x},t) = \boldsymbol{L}_\lambda \boldsymbol{U}(\boldsymbol{x}, t)-\boldsymbol{N}_\lambda \boldsymbol{U}(\boldsymbol{x}, t) \tag{3.2}$$

The control parameters $\lambda = (\lambda_1 , \lambda_2 , \ldots)$ describe the impact of the surrounding on the system, while internal or external fluctuations can cause dependence of λ on the time. $\boldsymbol{L}_\lambda$ is a linear operator and $\boldsymbol{N}_\lambda$ is a non-linear operator. A similar system of non-linear equations is found if instead of the fluid description, we use Boltzman-Vlasov model, where the fluid variables are substituted by distribution functions $f_a(\boldsymbol{x}, \boldsymbol{u}, t)$ for every kind of charged particles of plasma state. The essence of non-linear dynamics as we understand it, is the efficiency of non-linear systems to bring about spatial and temporal or functional structures on the macroscopic level. In particular as the control parameter λ change and the system moves away from equilibrium, its asymptotic motion gets more and more complicated through successive bifurcations at critical values of λ, while after amplification of stochastic fluctuations and development of instabilities, new spatial-temporal patterns can be revealed (Prigogine and Nicolis, 1985; Haken, 1988).

The general solution of the non-linear plasma equations at a bifurcation point λ_o is supposed to have the general form

$$\boldsymbol{U}(\boldsymbol{x}, t) =\boldsymbol{U}_0+\sum_j \xi_j(t)\, \boldsymbol{q}_j(\boldsymbol{x}) \tag{3.3}$$

where $q_j(x)$ are the spatial modes with eigenvalues λ_j according to linear stability analysis around the stable solution $\boldsymbol{U}_0$ (Haken, 1983; Spiegel, 1985). The variables $\xi_i(t)$ describe the infinite dimensional space state of the system. Through adiabatic approximation which leads to the slaving principle we can identify a finite number of order parameters $u_i \equiv \xi_i$ for which $Re\{\lambda_i\} > 0$. These are unstable (slow) modes which slave the stable {fast} modes

$s_j \equiv \xi_j$ with $Re\{\lambda_j\} < 0$, so that we may express $s_j(t)$ by $u_j(t)$, according to $s_j(t) = f\{u_i(t)\}$. That is, at critical points the plasma physical state $U(x,t) \equiv \{\xi_1(t), \xi_2(t), \dots\}$ moves asymptotically to finite dimensional subspace described by the order parameters $\{u_1(t), u_2(t), \dots\}$.

The development of spatial patterns as the system crosses the bifurcation points (or critical points) can be described by the order parameters $u_j(t)$ through the skeleton relations

$$U(x, t) = const + \sum_j u_j(t)\, q_j(x) \tag{3.4}$$

Generally the order parameters can be determined by certain nonlinear equations which are similar to Ginzburg-Landau equations (Haken, 1983). Different kinds of spatio-temporal patterns can occur after instability as the plasma system moves away from equilibrium. If we consider only temporal patterns we may find successively time-independent states (point attractor), periodic motion (limit cycle), quasiperiodic motion (torus) and finite dimensional turbulence (chaos with strange attractors) (Gaponov-Grekhov and Rabinovich, 1992).

In order from this general (scheme) to obtain physical realism we must use the appropriate boundary conditions. In the case of the magnetospheric plasma, if this general theory corresponds to a reality, some of the order parameters $u_i(t)$ correspond to unstable slow modes which constitute the macroscopic low dimensional phase space of the magnetospheric system satisfying the reduced system of equations with general form:

$$\frac{dx}{dt} = F(x(t), z(t)) \tag{3.5}$$

Now the vector $x(t)$ describes the internal dynamic state of the magnetospheric system in its macroscopical phase space, while $z(t)$ describes those order parameters which cause the coupling of the magnetospheric system with the solar wind system, and are named external control parameters. For the existence of low magnetospheric chaos, the flow $F(x, z)$ must be nonlinear. After this, especially for the variable x, the observation of the magnetospheric system through the AE index, the energetic particle densities etc. corresponds to an equation of the form

$$y(t) = h(x(t), z(t)) \tag{3.6}$$

where $y(t)$ is the measured magnetospheric variable. The system described by (3.5) and (3.6) is known as input-output system. Input-output systems constitute a crucial part of the general theory of dynamical systems. (Cook, 1994; Casdagli et al., 1992; Abarbanel et al., 1993), and they have been proposed for the modeling of the magnetospheric dynamics (Vassiliadis and Daglis, 1993; Vassiliadis and Klimas, 1995; Price et al., 1994; Prichard and Price, 1993; Klimas et al., 1996; 1997). Generally the input variable z(t) can be deterministic or stochastic, periodic or random. For the magnetospheric system the input variable $z(t)$ corresponds to dynamical variables of the solar wind system (velocity, magnetic field, density etc.) Moreover it is natural to suppose that the dynamical variables $x(t)$ and $z(t)$ contain stochastic components according to the relations

$$\begin{aligned} x(t) &= \langle x(t) \rangle + \delta x(t) \\ z(t) &= \langle z(t) \rangle + \delta z(t) \end{aligned} \tag{3.7}$$

where $\langle \bullet \rangle$ denotes the statistical mean value. The stochastic components δx and δz may be Gaussian white noise, non-Gaussian white noise or colored noise. In this case the equation (3.5) corresponds to a stochastic system with a possible expression

$$\frac{d\langle x \rangle}{dt} = F(\langle x \rangle, \langle z \rangle) + g(\langle x \rangle, \langle z \rangle, w(t)) \tag{3.8}$$

where F is the deterministic flow of the system and g is the stochastic diffusion. In the following we use the variables x, z to represent the mean values of the macroscopic order parameters. Generally $w(t)$ is a white noise signal since every colored noise can be transformed to a series of white noise under certain conditions (see paragraph *5.1*). The relation (3.8) corresponds to a general stochastic process and helps us to understand the importance of the criticism against the magnetospheric chaos as it was reviewed previously. That is the central problem of the magnetospheric dynamics is to understand the cause of the randomness of the observed magnetospheric magnitudes. Is the observed randomness of the magnetospheric magnitudes (as the AE index, the energetic particle densities etc.) caused by the stochastic components $g(x, z, w(t))$ in the above equation (3.8), or by the deterministic flow $F(x, t)$? In the second case the questions becomes as follows. Is the magnetospheric randomness caused externally by the random input variable $z(t)$ or by the sensitivity to the initial conditions of the deterministic flow F even if the input variables remain constant? Moreover if the magnetospheric signals reveal non-linearity and low-dimensionality, which is the cause? Are these characteristics caused by the input variable $z(t)$ or by the form of the deterministic flow F which describes the internal dynamics of the magnetospheric system? As we show in the next sections the modeling of the magnetospheric dynamics by the equation (3.8) is the basis for the nonlinear analysis of experimental time series.

In answering the above questions by using experimental observations we must decide upon the deterministic flow $F(x, z)$ in (3.8) as follows:

a) it is infinite dimensional or low dimensional
b) it is linear or non-linear and in which term between

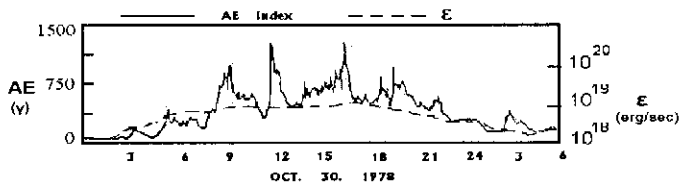

Fig. 1. The AE index (solid line) and the solar wind energy input function E (dashed line) during October *30, 1978*. Energy input remains fairly constant for about *12* hours while the AE index reveals several impulsive changes. The AE index also reveals an enhanced level component which follows the energy input and is directly driven by the solar wind.

internal state variable x and the input variable z

c) if it is non-linear in the state variable x then the evolution in the phase space is periodic or chaotic.

In addition concerning the input variable z we must decide upon its influence on the dynamics of the magnetospheric system, as well as upon its influence on the experimentally observed magnetospheric variables $y(t)$ according to (3.6). Finally we must decide upon the function $h(x, z)$ in (3.6) if it is linear or nonlinear and in which term. Although at this stage of research it is not possible to answer all these questions, however in the following we try to clarify them.

4. Solar wind and magnetosphere interaction

In magnetospheric dynamics there is a ground state of the magnetosphere during quite times. Energization of the magnetosphere above the ground state can be observed when the interplanetary magnetic field shifts from northward to southward and the magnetic merging at the subsolar magnetopause is identified. The expansion phase is the result of an explosive release of energy stored in the geomagnetic tail (McPherron, 1979; Klimas et al., 1996). A substorm features two distinctly different components of activity. The first component corresponds to the externally driven activity and reflects the direct deposition of energy from the solar wind to regions of the high latitude ionosphere. The second component of the substorm dynamics corresponds to a random sequence of events related to stored energy release and is known as loading-unloading or storage-release process (Rostoker, 1991). The Earth's magnetotail is the space where the inward energy is stored. Therefore if low-dimensional chaos has something to do with magnetospheric dynamics this is due to the second process, that is the loading-unloading process that could be chaotic. The first kind of process known as the driven deposition of energy is weakly related to the internal dynamics of the magnetosphere and it can be supposed to be a linear process. Oppositely the loading – unloading process is a more synthetic process including a series of connected plasma phenomena in the magnetospheric magnetotail (McPherron, 1979). This kind of magnetospheric processes has been testified by an existing rich phenomenology of the magnetospheric substorms which are assumed to be nonlinear and chaotic, as it has been also supported by theoretical studies, (Baker et al., 1990; Klimas et al., 1991, 1992; Pavlos et al., 1994; Klimas et al., 1996; 1997). This point of view is verified by the study of isolated substorm events which reveal that the AE index consists of two distinct components. The one component corresponds to the driven process and it is manifested as smooth increase and decrease of the AE index with clear correlation to the solar wind changes. The other component corresponds to unpredictable and repeatable burst of AE index to high values. The second component is related to the inner magnetospheric dynamics which is not driven externally and can be a chaotic unloading of the stored energy. This mixing of two different characteristics of the magnetospheric dynamics becomes a source of obscurity for the experimental verification of magnetospheric chaos by using only the AE index time series.

Already Lee et al. (1985) examined the magnetospheric system and the interplanetary space for the day October *30, 1978*, during which the energy input (E) remained fairly constant at high values for about 12 hours as shown in Fig. 1. As we can see in this figure during the period that there is strong coupling between the solar wind and the magnetosphere ($E>10^{18}$ erg/sec) there is an smoothly enhanced level component of the AE index as well as a randomly impulsive component associated with auroral substorms as it was described previously. In Fig. 1 we can see that as the rate of energy flow remains constant at $\sim 10^{18}$erg/sec substorm events can be observed in a random way. According to Lee et al. (1985) the smoothly enhanced level of AE index is directly driven by the solar wind through the enhancement of the polar cap potential drop, while the random and impulsive component is related to the repeated occurrence of plasmoids in the magnetotail. The last process is undriven and corresponds to the internal magnetospheric dynamics according to the previous description. Price and Prichard (1993) have also studied the same day with the follow remark: *"Although the magnetosphere is not autonomous system, when the input forcing function is relatively steady the system may have time to converge to an attractor"*. The above experimental event as well as other results (Pavlos et al., 1994; 1999a,b) are in an excellent agreement with the general concept of chaos for a nonlinear low dimensional system as it will be described below.

Let us consider the solution $x=x(t)$ of the differential nonlinear equation system described by the vector field $F(x, \lambda)$, according to the autonomous equation

$$\frac{dx(t)}{dt} = F(x(t), \lambda) \tag{4.1}$$

which describes the dynamics of a physical system with initial condition $x(0)=x_0$ corresponding to the ground state of the system. We are interested in the behavior of $x(t)$ as $t \to \infty$. In the general situation F depends on some physical parameter λ which describes the external perturbation and the coupling of the system with other physical systems. The variable $x(t)$ belongs to the phase space of the system which is the $\mathbf{R}^n$ space in the finite-dimensional case and a Hilbert space in the infinite-dimensional case. In general, for small λ, there exists a unique stationary solution which corresponds to a thermodynamical equilibrium of the system. When λ gets larger, then something similar to a Hopf bifurcation can occur in time periodic and quasi-periodic solutions. Finally, for large values of λ, chaos can be observed where $x(t)$ looks completely random for all time and a Fourier analysis leads to a wideband continuous spectrum. This corresponds to the phenomenon of turbulence from the dynamical point of view. Of course the above scenario of the sequence of transient states being similar with turbulence is very schematic while the situation can be more complicated. (Argyris et al., 1994; Hao Bai-Lin, 1984; Teman, 1988).

However the modeling of the magnetospheric dynamics as it was described in section *3* (relations (3.5)-(3.8)) reveals that the magnetospheric system behaves as a non-autonomous system. This can create doubts about the importance of the previous description as a possible road to magnetospheric chaos (rel. *4.1*) and create problems with the physical meaning of nonlinear analysis of magnetospheric time series by using embedding methods (see the following paragraph 5.2) (Takens, 1981). As we have noticed in Fig. 1 the crucial parameter for the description of the solar wind–magnetosphere coupling is the energy input function $E(t)$ which can be expressed as function of the input (solar wind) variables such as, the interplanetary magnetic field (IMF) B or the solar wind bulk velocity V. Furthermore according to the above description, part of this energy is directly deposited in polar cap and the rest is deposited in the earth's magnetotail. The second process corresponds to the magnetotail dynamo and causes the cross-tail potential drop which is given by the relation

$$\Phi_{CT} = B_n V_{sw} L_w \tag{4.2}$$

where B_n is the normal component of the magnetic field on the tail magnetopause, V_{sw} is the solar wind speed near to the tail magnetopause and L_w is the width of the open magnetotail. Φ_{CT} is the external electric motive force (driving force) and a typical value of which is *20 kV* during quite times and *100-150 kV* during substorms (Liu et al., 1988; Klimas et al., 1992, 1996; Pavlos et al., 1994, Baker et al., 1995; Vassiliadis and Klimas, 1995). The IMF B and the solar wind bulk velocity V constitute the main components of the external input parameters z for the magnetospheric system, while the energy input $E(t)$ or the cross potential drop Φ_{CT} are functions of these input variables (Acasofu, 1981.). Therefore the control parameter λ included in (4.1) in the case of the magnetospheric system depends upon time and coincides with the solar wind input variables z. In the next sections we develop an appropriate strategy in order to study the magnetospheric dynamics by using experimental time series especially from the point of view of the questions raised in the last part of the previous section as well as in relation to the solar wind input variables z. We must also note that the external driving force Φ_{CT} of the magnetospheric system is a random variable because the solar wind variables B and V reveal random behaviors (Pavlos et al., 1992a,b).

5. The concepts of linearity, non-linearity and dimensionality in the modern analysis of time series

The main purpose of time series analysis is to extract significant information for the underlying dynamics of the observed signal, as well as to develop effective methods for modeling and prediction. Classical time series analysis confronts these problems by using linear or nonlinear input-output methods (Priestley, 1988). On the other hand the modern analysis of time series which is named chaotic analysis includes: a) Estimation of the geometrical and dynamical characteristics of the trajectory of the system in its phase space (Pavlos et al., 1999a,b, Abarbanel et al., 1993; Grassberger and Procaccia, 1983; Tsonis, 1992) b) Testing techniques for the discrimination of low-dimensional non-linear determinism and linear stochastic processes (Provenzale et al., 1992; Theiler, 1991; Theiler et al., 1992a,b, 1993). c) Forecasting algorithms (Gasdangli et al., 1991; Farmer and Sidorowich, 1987; Weigend and Gershenfeld, 1994). The above chaotic algorithm have been applied recently for the magnetospheric AE index by Pavlos et al. (1999a, b).

5.1 Classical analysis of time series and input-output systems

The fundamental theorem of classical time series analysis lies on the Wold decomposition theorem (Priestly 1988; Tong 1990; Theiler et al., 1993). According to this theorem any stationary process with continuous power spectrum can be described by an autoregressive moving average model of the form

$$y(t) = y_o + \sum_{i=1}^{\infty} b_i\, y\,(t-i) + \sum_{i=1}^{\infty} g_i \varepsilon(t-i) \tag{5.1}$$

The first sum corresponds to a deterministic linear process $D(t)$ with finite or (possibly infinite) combination

of past values. The second sum corresponds to a probabilistic process $R(t)$ and is written as an infinite sequence of random uncorrelated white noise variables $\varepsilon(t)$. It can be shown that the autocorrelation function C_D of the deterministic component of time series will be nonzero for large lagtime while for the probabilistic component, the autocorrelation C_R decays to zero sufficiently fast (Theiler et al., 1993). Moreover, if $\{e(t)\}$ constitutes a sequence of independent random variables, then the random process $R(t)$ underlying the time series is of infinite dimension. However when $\{e(t)\}$ is not a sequence of independent random variables, then it is possible to exist a function $h\{.\}$ such that

$$h(y_t, y_{t-1}, \ldots, y_{t-d}) = e_t \tag{5.2}$$

where $\{e_t\}$ is a strict white noise (Priestley, 1988) The index $(t-d)$ must be near the decorrelation time of the time series. The function $h\{.\}$ describes the underlying deterministic dynamics of the system and may be linear or nonlinear. Therefore using (5.1) and (5.2) we obtain a Markov process as follows

$$\boldsymbol{x}_{t+1} = \boldsymbol{F}(x_t, e_t, e_{t+1}) \tag{5.3}$$

where $\boldsymbol{x}_t$ and $\boldsymbol{e}_t$ denote the vectors

$$\boldsymbol{x}_t = (y_t, \ldots, y_{t-d+1}) \quad \boldsymbol{e}_t = (e_{t-d}, \ldots, e_{t-k}) \tag{5.4}$$

and $\boldsymbol{x}_t$ corresponds to the reconstructed state of the underlying system in a d-dimensional state space. The function $\boldsymbol{F}$, can be linear or nonlinear and include the dynamical and stochastic components of the underlying random process (Priestley, 1988; Tong, 1990). The state $\boldsymbol{x}_t$ of the d-dimensional system is related to the observed time series by a relation

$$y_t = \boldsymbol{H}(y_t, \ldots, y_{t-d+1}; e_{t-1}, \ldots, e_{t-k}) + e_t \tag{5.5}$$

(Priestley, 1988). The Markov process defined by (5.3) reflects the dynamics of the physical system contained in the observed time series $y(t)$. When the underlying physical system is non-autonomous then there must exist an external forcing or input time series $z(t)$ according to the (3.6). The external driving $z(t)$ can also be described by an autoregressive moving average model in accordance with the Wold decomposition theorem. In this case (5.3) and (5.5) can be extended and are written as a general input-output stochastic process of the form

$$\boldsymbol{x}_{t+1} = \boldsymbol{F}(\boldsymbol{x}_t, \boldsymbol{z}_t, \boldsymbol{e}_t, \boldsymbol{e}_{t+1}) \tag{5.6}$$

$$y_t = H(\boldsymbol{x}_t, \boldsymbol{z}_t, \boldsymbol{e}_t) + e_t \tag{5.7}$$

where $\boldsymbol{x}_t = (x_t, \ldots, x_{t-d+1})$ corresponds to the d-dimensional internal state of the system; $\boldsymbol{z}_t = (z_t, \ldots, z_{t-m+1})$ is the m-dimensional input and e_t is the purely stochastic component. Therefore according to the classical theory of time series every experimental signal, which reveals a) stationarity and b) autocorrelation function decaying to zero must be related to a dynamical system perturbed by a stochastic white noise. When the deterministic component $\boldsymbol{F}$ is low-dimensional and non chaotic, then the stochastic component constitutes the main cause of the broadband spectrum and makes the autocorrelation function to show short time decay. On the other hand, when the deterministic component is chaotic or high dimensional then the determinism can cause the same characteristics on the power spectrum and the autocorrelation function. However the classical time series theory cannot help us to extract significant information about the deterministic component, especially when the function $\boldsymbol{F}(x)$ is nonlinear. In contrast the chaotic analysis of time series based on the embedding theory, permits us to extract useful results about the deterministic component $\boldsymbol{F}(x)$.

5.2 Embedding theory and time series analysis.

The embedding theory permits one to study the dynamical characteristics of a physical system by using experimental observations in the form of time series (Takens, 1981; Broomhead and King, 1986). Let $\boldsymbol{x}(t) = f^{(t)}(\boldsymbol{x}(0))$ denote the dynamical flow underlying an experimental time series $x(t_i) = h(\boldsymbol{x}(t_i))$ where h describes the measurement function. When there is a noisy component $w(t_i)$ then the observed time series must be given by $x(t_i) = h(\boldsymbol{x}(t_i), w(t_i))$. On the other hand Takens (1981) showed that for autonomous and purely deterministic systems the delay reconstruction map $\boldsymbol{\Phi}$, which maps the states $\boldsymbol{x}$ into m-dimensional delay vectors

$$\boldsymbol{\Phi}(\boldsymbol{x}) = [h(\boldsymbol{x}),\ h(f^{\tau}(\boldsymbol{x})),\ h(f^{2\tau}(\boldsymbol{x})), \ldots,\ h(f^{(m-1)\tau}(\boldsymbol{x}))] \tag{5.8}$$

is an embedding when $m \geq 2n+1$, where n is the dimension of the manifold $\boldsymbol{M}$ of the phase space in which evolves the dynamics of the system. This means that interested geometrical and dynamical characteristics of the underlying dynamics in the original phase space are preserved invariable in the reconstructed space al well.

Let $\boldsymbol{X}_r = \boldsymbol{\Phi}^{(t)}(\boldsymbol{X})$ be the reconstructed phase space and $\boldsymbol{x}_r(t_i) = \boldsymbol{\Phi}(\boldsymbol{x}(t_i))$ the reconstructed trajectory for the embedding $\boldsymbol{\Phi}$. Then the dynamics evolved in the original phase space is topologically equivalent to its mirror dynamical flow in the reconstructed phase space according to

$$f_r^t(\boldsymbol{x}_r) = \boldsymbol{\Phi}(x) \circ f^t(\boldsymbol{x}) \circ \boldsymbol{\Phi}^{-1}(\boldsymbol{x}_r) \tag{5.9}$$

of the reconstructed phase space $\boldsymbol{X}_r$. In other words the embedding $\boldsymbol{\Phi}$ is a diffeomorphism which takes the orbits

$f^t(x)$ of the original phase space to the orbits $f_r^t(x_r)$ in the reconstructed phase in such a way of preserving their orientation and other topological characteristics as eigenvalues, Lyapunov exponents or dimensions of the attractors. According to the above theory, in the reconstructed phase space we can estimate geometrical characteristics as dimensions, which correspond to the degrees of freedom of the underlying dynamics of the experimental time series ,as well as dynamical as Lyapunov exponent, mutual information and predictors (Pavlos et al., 1999a,b). In the next sections we show that embedding theory can be also applied for non-autonomous or stochastic systems fruitfully.

5.3 Chaoticity versus stochasticity

Many authors have also supported the view that stochastic time series (colored noises) can produce in many cases the profile of chaotic systems revealing low correlation dimensions or positive Lyapunov exponents without the underlying physical system to be really chaotic, (Osborne et al., 1986; Provenzale et al., 1992; Theiler et al., 1991; Theiler et al., 1992a,b;). Also, according to Theiler the concept of correlation dimension can be applied in two quite distinct ways to the time series analysis: (i) to indicate the number of degrees of freedom in the underlying dynamical system, and (ii) to quantify the self-affinity or crinklesness of the trajectory in the reconstructed phase space (Theiler et al., 1991). In the second case, more crucial than the high frequency crinkles is whether or not the trajectory is recurrent through phase space. For a non recurrent colored noise the dimension of the full trajectory will be equal to the dimension of a local segment, while for a recurrent colored noise (if the time series is long enough to be recurrent) the estimated correlation dimension will be that of the embedding space. For this reason and in order to exclude the case of signals without recurrent character in the reconstructed phase space we restrict our estimations of the correlation integral to time uncorrelated reconstructed states $x(t_i)$, $x(t_j)$ according to $|i-j| > w$ with values of w higher than the decorrelation time series. This means that we exclude all the correlated pairs included in a sphere with diameter $2w$. The parameter w was introduced by Theiler and is named as Theiler parameter. The exclusion of time correlated pairs must leave invariant the estimated value of the correlation dimension and other magnitudes if the underlying process of the observed signal is low-dimensional. However the above test of Theiler can not help to decide about the linearity-nonlinearity and chaoticity of the underlying process. The stochastic component of a time series can increase the Lyapunov exponents, causing some of them to be positive, while the underlying deterministic process have no positive Lyapunov exponent (Argyris et al., 1998). Also it is possible for an original time series which is related to a linear process to obtain nonlinear characteristics after a nonlinear static distortion. In order to decide upon these questions we can use the method of surrogate data (Theiler et al., 1992a,b; Schreiber and Schmitz, 1996). According to this method we compare every result estimated in the reconstructed phase space with similar result estimated for stochastic time series which mimic the original in respect to the autocorrelation function and the amplitude distribution. For the magnetospheric time series of the AE index we have used the above tests and we have obtained significant evidence for low dimensionality, non-linearity and chaoticity (Pavlos et al., 1999a,b).

5.4 Input- output methods

In the case of non-autonomous systems, as the magnetospheric system is observed to be the chaotic analysis of experimental time series must be related to the general concept of input-output dynamical processes. That is, for non-autonomous dynamical system, it is not clear if the estimated geometrical and dynamical characteristics of an experimental time series (as correlation dimension, Lyapunov exponents and nonlinearities) correspond to the internal dynamics of the system or to the external coupling. In addition, for non-autonomous dynamical systems it is difficult to decide which characteristics of the system belong to the system itself and which are caused by the external input of the system. In order to confront this problem for the case of the magnetospheric system we follow three independent strategies: a) We consider the input variable as a external noise which perturbs the magnetospheric dynamics. b) We consider the input variable as an aperiodic external driving. c) We consider the input variable as a time varying control parameter of an autonomous system. In any one of the above strategies the internal dynamics can be supposed to be linear or non-linear, low or high dimensional, chaotic or periodic, deterministic or stochastic in accordance to the theoretical description of the previous sections. Also in the case of nonlinear internal dynamics the input variable can be coupled with different kinds of possible internal dynamics as: limit point, limit torus or strange attractors. Therefore the crucial point is to decide if the magnetosphere includes an internal rich dynamics and of which kind, or if the magnetosphere constitutes a passive filtering of the external (solar wind) dynamics, by applying the chaotic analysis on the magnetospheric signals. In the last case it is possible to think that the chaotic profile of the magnetospheric time series does not correspond to real magnetospheric chaos but to an appropriate magnetospheric filtering of the solar wind input variables. A special kind of filtering can be obtained by linear recursive filters of finite order:

$$y(t) = \sum_{i=0}^{n} a_i\, z(t-i) + \sum_{i=1}^{n} b_i y(t-i) \qquad (5.10)$$

(Broomhead et al., 1992). In the above relation $z(t)$, $y(t)$ are the input and output signals and $\{a_i\}$, $\{b_i\}$ are sets of real parameters which define the filters. The term recursive means the existence of a_i, $b_i \neq 0$ which implies that the delayed output of the filter is fed back into the input. When the parameters $\{b_i\}$ are functions of the output signal, then we have nonlinear filtering. The recursive character of a filter implies an internal dynamics of the filter which can be linear or nonlinear. From this point of view the recursive filtering corresponds to a general dynamical process perturbed by the external input $z(t)$. However this permits us to apply the above three strategies for non-autonomous input-output systems in order to study the influence of the input on the recursive component of the filter. A general recursive filter (linear or nonlinear) can change the dimension of the input signal in a definite way which is studied in the following section *6*. For linear and non-recursive filtering it can be proved that the correlation dimension of the input signal remains invariant (Broomhead et al., 1992). In this kind of filters belong the low pass filters which are used for the noise reduction. Such filters are moving average, wavelet or SVD filters (Abarbanel et al., 1993; Broomhead and King, 1986). Non-linear and non-recursive filters correspond to static distortion of the input signal which can change its dimension and transform a linear to a non-linear signal. So this case of filtering can be studied by the method of surrogate data. As we have previously noticed this method permits us to exclude the possibility that the output signal is a static distortion of an linear input signal. The above described recursive filters constitute an approximation of general infinite impulse response (IIR) filters. IIR filters can be described by a Voltera series:

$$y(t) = \sum_{i=0}^{\infty} a_i z(t-i) + \sum_{i=0}^{\infty}\sum_{j=0}^{\infty} g_{ij} z(t-i)z(t-j) + \ldots \qquad (5.11)$$

(Priestley, 1988) Supposing a deterministic law of the form

$$H(\ldots y(t-1), y(t-2), \ldots, z(t), z(t-1), z(t-2)\ldots) \cdot y(t) \qquad (5.12)$$

between the input and the output signals, which corresponds to the internal dynamics of the filter then *(5.12)* can be written as a general input-output recursive relation

$$y(t) = \sum_{i=0}^{\infty} a_i z(t-i) + \sum_{i=0}^{\infty} b_i y(t-i) + \sum_{i=0}^{\infty}\sum_{j=0}^{\infty} q_{ij} z(t-i)z(t-j) + \sum_{i=0}^{\infty}\sum_{j=0}^{\infty} b_{ij} y(t-i)y(t-j) + \ldots \qquad (5.13)$$

The last relation reveals the existence of an internal dynamical process of the filter as well. The recursive component corresponds to the internal dynamical component and can cause the change of the dimension and other characteristics of the signal.

The above description of the filtering process constitutes an application of the general system theory which is summarized in the equation

$$\frac{d\boldsymbol{x}}{dt} = \boldsymbol{f}(\boldsymbol{x}(t), \boldsymbol{u}(t), t) \qquad (5.14)$$

for the continuous time systems and

$$\boldsymbol{x}(t+1) = \boldsymbol{f}(\boldsymbol{x}(t), \boldsymbol{u}(t), t) \qquad (5.15)$$

for discrete-time systems (Cook, 1994).

5.5 Singular value analysis

Singular value analysis has been proved to be a strong and effective method for modern time series analysis. It was used by Broomhead and King (1986) for first time and comes from the generalized theory of information. In this study we use the above analysis in two cases: (i) as a time series filter and (ii) to decompose a time series in the deterministic components which can be used for the detection of the underling dynamics. Singular value analysis is applied to the trajectory matrix which is constructed by an experimental time series as follows:

$$X = \begin{bmatrix} x(t_1), (t_1+\tau), \ldots x(t_1+(n-1)\tau) \\ x(t_2), x(t_2+\tau), \ldots x(t_2+(n-1)\tau) \\ \cdot \quad \cdot \quad \cdots \quad \cdot \\ x(t_N), x(t_N+\tau), \ldots x(t_N+(n-1)\tau) \end{bmatrix} = \begin{bmatrix} \boldsymbol{x}_1^T \\ \boldsymbol{x}_2^T \\ \cdot \\ \boldsymbol{x}_N^T \end{bmatrix} \qquad (5.16)$$

where $x(t_i)$ is the observed time series and τ is the delay time for the phase space reconstruction. The rows of the trajectory matrix constitute the state vectors $\boldsymbol{x}_i^T$ on the reconstructed trajectory in the embedding space R^n. As we have constructed N state vectors in embedding space R^n the problem is how to use them in order to find a set of linearly independent vectors in R^n which can describe efficiently the attracting manifold within the phase space according to the theoretical concepts of paragraph *5.2*. These vectors constitute part of a complete orthonormal basis $\{e_i, i=1,2,..n\}$ in R^n and can be constructed as a linear combination of vectors on the reconstructed trajectory in R^n by using the relation

$$\boldsymbol{s}_i^T \boldsymbol{X} = \sigma_i \boldsymbol{c}_i^T \qquad (5.17)$$

According to singular value decomposition (SVD) theorem it can be proved that the vectors s_i and c_i are eigenvectors of the structure matrix XX^T and the covariance matrix X^TX of the trajectory according to the relations

$$XX^T s_i = \sigma_i^2 s_i, \quad X^TX c_i = \sigma_i^2 c_i \tag{5.18}$$

(Brogan, 1982). The vectors s_i, c_i are the singular vectors of X and σ_i are its singular values, while the SVD analysis of X can be written as

$$X=S\Sigma C^T \tag{5.19}$$

where $S = [s_1, s_2, \ldots s_n]$, $C = [c_1, c_2, \ldots c_n]$ and $\Sigma = diag[\sigma_1, \sigma_2, \ldots \sigma_n]$. The ordering $\sigma_1 \geq \sigma_2 \geq \ldots \geq \sigma_n \geq 0$ is assumed. Moreover according to the SVD theorem the non-zero eigenvalues of the structure matrix are equal to non-zero eigenvalues of the covariance matrix. This means that if n' (where $n' \leq n$) is the number of the nonzero eigenvalues, then $\text{rank}XX^T = \text{rank}X^TX = n'$. It is obvious that the n'–dimensional subspace of R^N spanned by $\{s_i, i=1,2,\ldots n'\}$ is mirrored to the basis vector c_i which can be found as the linear combination of the delay vectors by using the eigenvectors s_i according to *(5.17)*. The complementary subspace spanned by the set $\{s_i, i=n'+1,\ldots N\}$ is mirrored to the origin of the embedding space R^n according to the same relation *(5.17)*. That is according to SVD analysis the number of the independent eigenvectors c_i that are efficient for the description of the underlying dynamics is equal to the number n' of the non-zero eigenvalues σ_i of the trajectory matrix. The same number n' corresponds to the dimensionality of the subspace containing the attracting manifold. The trajectory can be described in the new basis $\{c_i, i=1,2,\ldots n\}$ by the trajectory matrix projected on the basis $\{c_i\}$ given by the product XC of the old trajectory matrix and the matrix C of the eigenvectors $\{c_i\}$. The new trajectory matrix XC is described by the relation

$$(XC)^T(XC) = \Sigma^2 \tag{5.20}$$

This relation corresponds to the diagonalization of the new covariance matrix so that in the basis $\{c_i\}$ the components of the trajectory are uncorrelated. Also, from the same relation *(5.20)* we conclude that each eigenvalue σ_i^2 is the mean square projection of the trajectory on the corresponding c_i, so that the spectrum $\{\sigma_i^2\}$ includes information about the extending of the trajectory in the directions c_i as it evolves in the reconstructed phase space. The explored by the trajectory phase space corresponds on the average to an n-dimensional ellipsoid for which $\{c_i\}$ give the directions and $\{\sigma_i\}$ the lengths of its principal evolves in the subspace spanned by eigenvectors $\{c_i\}$

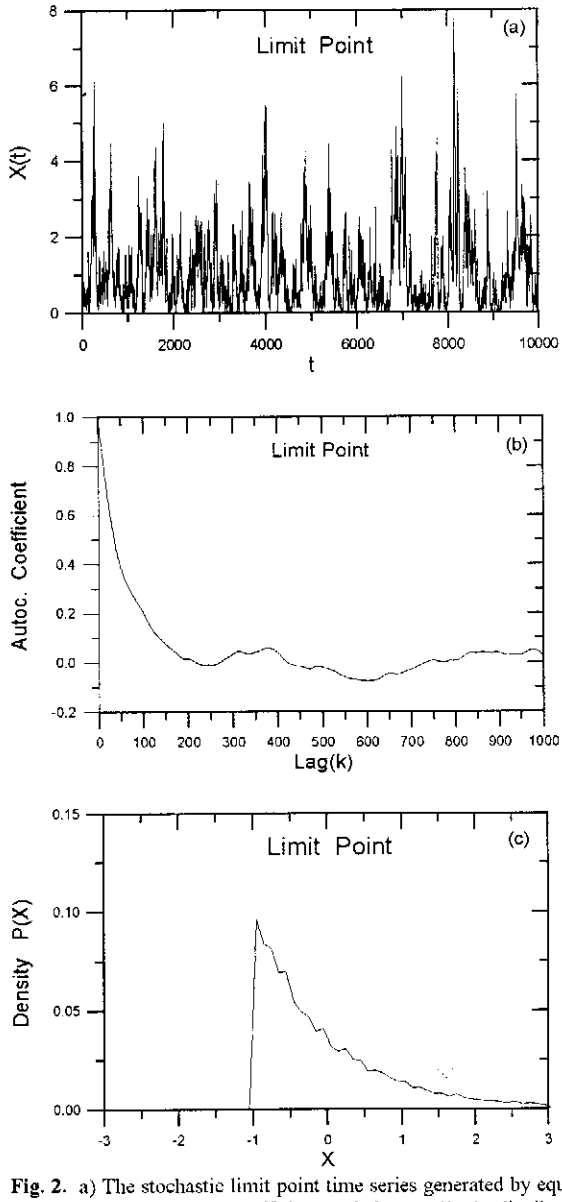

Fig. 2. a) The stochastic limit point time series generated by equation *(6.1)*. b,c) The autocorrelation coefficient and the amplitude distribution for the limit point time series.

corresponding to non-zero eigenvalues. However when the system is perturbed by external noise or deterministic external input then the trajectory begin to be diffused also in directions corresponding to zero eigenvalues where the external perturbation dominates. As we show in the following the replacement of the old trajectory matrix X with the new XC works as a linear low pass filter for the entire trajectory. Moreover the SVD analysis permits to reconstruct the original trajectory matrix by using the XC matrix as follows

$$X = \sum_{i=1}^{n} (Xc_i)c_i^T \tag{5.21}$$

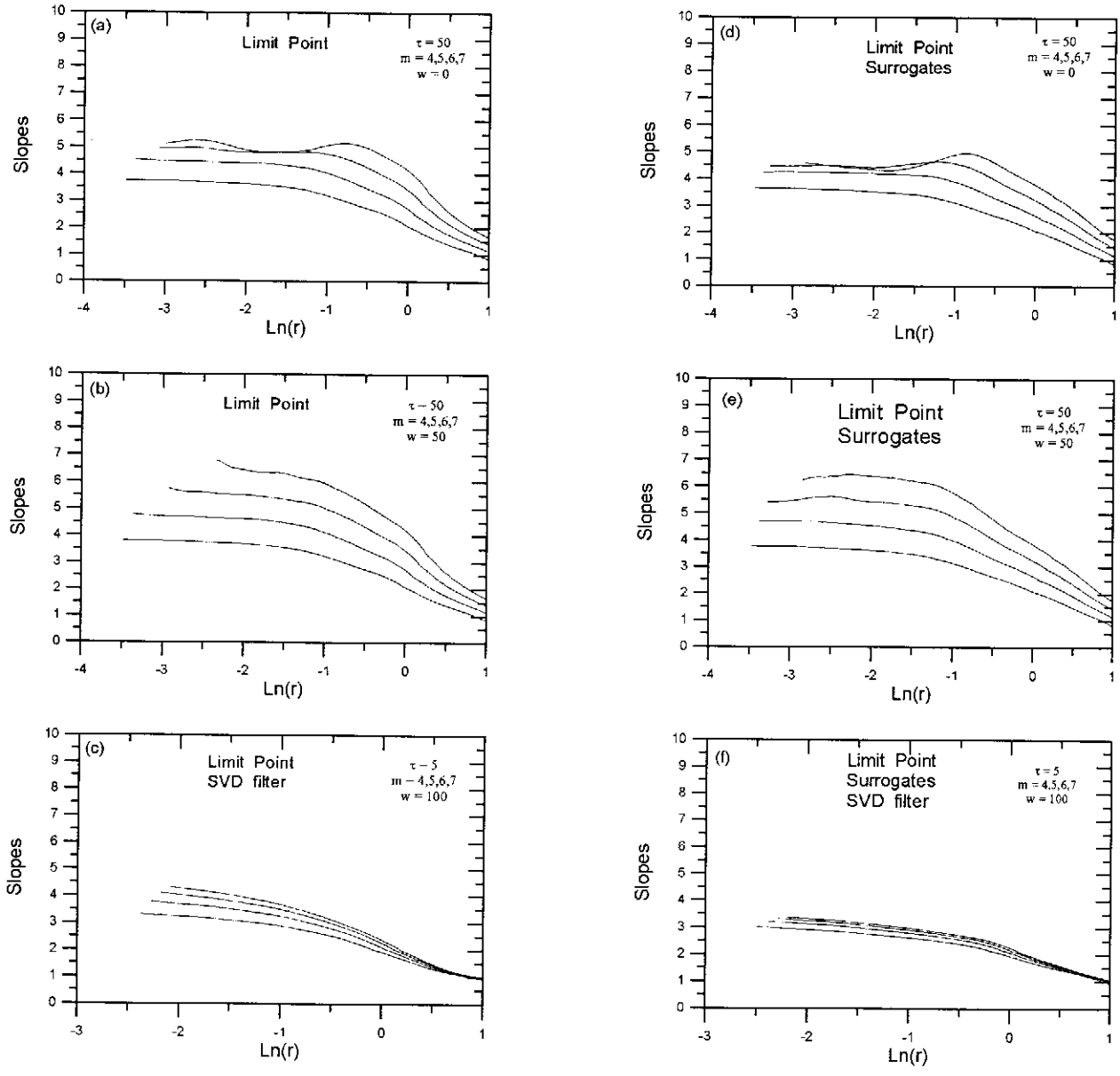

Fig. 3. a) The slopes of the correlation integrals as functions of radius for embedding $m=4,5,6,7$, Theiler parameter $w=0$, delay $\tau=50$, estimated for the stochastic limit point time series shown in Fig. 2a. The delay time $\tau=50$ corresponds to the best scaling profile of the correlation integrals with the best plateau. b) The same with *(a)* for $w=50$. c) The same with *(a)* but for $\tau=5$ and $w=100$, estimated for time series of Fig. 2a, when an SVD filter was used. d,e) The same with *(a)* corresponding to the surrogate data of the stochastic limit point time series but for $w=0$ and $w=50$ respectively f) The same with *(c)* but for the surrogate data.

The part of the trajectory matrix which contains all the information about the deterministic trajectory, as it can be extracted by observations corresponds to the reduced matrix:

$$\boldsymbol{X}_d = \sum_{i=1}^{n'} (\boldsymbol{X}\boldsymbol{c}_i)\boldsymbol{c}_i^T \tag{5.22}$$

which is obtained by summing only for the eigenvectors c_i with non-zero eigenvalues. From the relations *(5.21)* and *(5.22)* we can reconstruct the original time series $x(t)$ by using n new time series $v(t_i)$ according to

$$x(t) = \sum_{i=1}^{n} v_i(t) \tag{5.23}$$

where every $v_i(t)$ is given by the first column of the matrix $(\boldsymbol{X}\boldsymbol{c}_i)\,\boldsymbol{c}_i^T$. This is a kind of n-dimensional spectral analysis of a time series. An SVD filter of the original time series is also given by conserving only the components $v_i(t)$ corresponding to eigenvectors with σ_i greater than the noise floor. In this way we can obtain the deterministic component

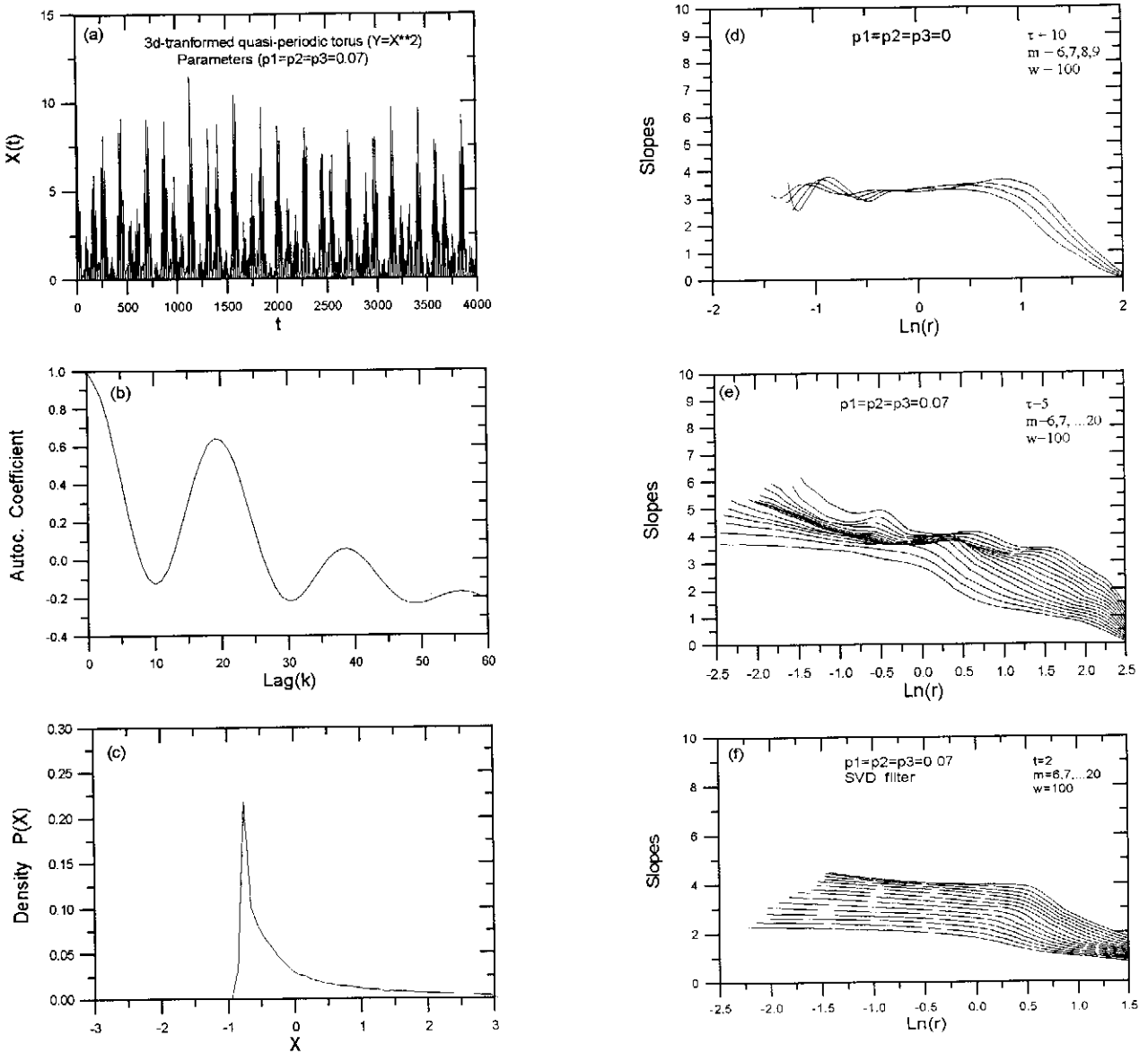

Fig. 4. a) The 3-dimensional quasi-periodic torus time series generated by equation *(6.4)* for stochastic coupling with $p_1=p_2=p_3=0.07$ and for a nonlinear transformation obtained by the relation $y=x^2$. b,c) The autocorrelation coefficient and the amplitude distribution estimated for the time series shown in *(a)*. d) The slopes of the correlation integrals for $m=6,7,8,9$, $w=100$, $\tau=10$, corresponding to the time series generated by equation *(6.3)* without stochastic perturbation. e) The same with *(d)* for the stochastic signal shown in *(a)*. f) The same with *(e)* but for the signal shown in Fig. (a) after an SVD filter was used.

$$X_d = \sum_{i=1}^{n'} v_i(t) \tag{5.24}$$

of the original time series $x(t)$.

6 Stochastic and deterministic input-output systems in relation to the magnetospheric dynamics.

6.1 Stochastic systems

According to *(3.8)*, *(5.3)-(5.10)* the magnetospheric system in any case includes an internal dynamics which can be perturbed by an input signal. In the following we suppose that the internal dynamics can be: a) a limit point b) a torus c) a strange attractor. In addition the input can be supposed to be deterministic or stochastic. In order to test every kind of dynamics we construct stochastic and deterministic input-output systems corresponding to the above three possibilities in such a way that their output signals mimic the magnetospheric signals in accordance with the autocorrelation function and the amplitude distribution. This analysis permits us to decide upon the nature of the magnetospheric system by comparing the above systems and their outputs with the magnetospheric system.

6.1.1 Limit point dynamics

In section *4* was described that, when the input energy E in the magnetosphere is constant and at low values ($E<10^{18}$ erg/sec), then the magnetospheric system remains in a stationary ground state. This makes us to suppose that the magnetospheric system might be some kind of dissipative oscillator which is externally perturbed in a random way. More generally, we can suppose that magnetospheric dynamics corresponds to the simple dynamics of limit point with random external impulse. Fig. 2a shows the time series obtained by a nonlinear stochastic process given by

$$\frac{dy}{dt} = (a - 0.5)b - y(t) + \left(2by(t)\right)^{\frac{1}{2}} w(t) \qquad (6.1)$$

where $w(t)$ is a standard Gaussian white noise process (Provenzale et al., 1991). For $w(t)$ equal to zero the deterministic component of the above system includes a limit point solution. The stochastic component does not permit the solution to be stabilized, creating a random nonlinear process with similar profile as the magnetospheric time series shown in the next section. Figs. 2(b-c) show the autocorrelation function and the amplitude distribution of the above signal. As we can see in these figures the signal decorrelates after ~ 250 units of lag time while its probability density is clearly non Gaussian, having a form between exponential distribution and F-distribution (Chua et. al., 1990). Fig. 3a shows the slopes of the correlation integral for the stochastic limit point time series when in the estimation of the slopes we do not exclude time correlated states in the reconstructed phase space, and we set the Theiler parameter $w=0$. There is a saturation of the slopes at the value $D \cong 5$. When we exclude the time correlated states the saturation profile is destroyed as we can see in Fig. 3b. Fig. 3c is similar with the above figures but an SVD filtering was applied on the original signal. Now, although the SVD filter presses the slopes to lower values than those of Fig. 3b, there is no significant saturation of the slopes. Also there is no significant scaling character of the correlation integrals as there is not an apparent plateau profile of the slopes. These results reveal that there is no dynamic low-dimensionality in the time series which was derived by the external perturbation of a limit point dynamics. Figs. 3(a-f) are similar to Figs. 3(a-c) and correspond to the surrogate signal constructed by the method Schreiber (Schreiber and (Schreiber and, Schmitz 1996; Pavlos et al., 1999a,b) with the same power spectrum and amplitude distribution as the original data shown in Fig. 2a. It becomes clear that there is no significant difference between the slopes of the original signal and its surrogate data. This means that the original signal is a purely stochastic signal caused by the original internal dynamics of the limit point which is

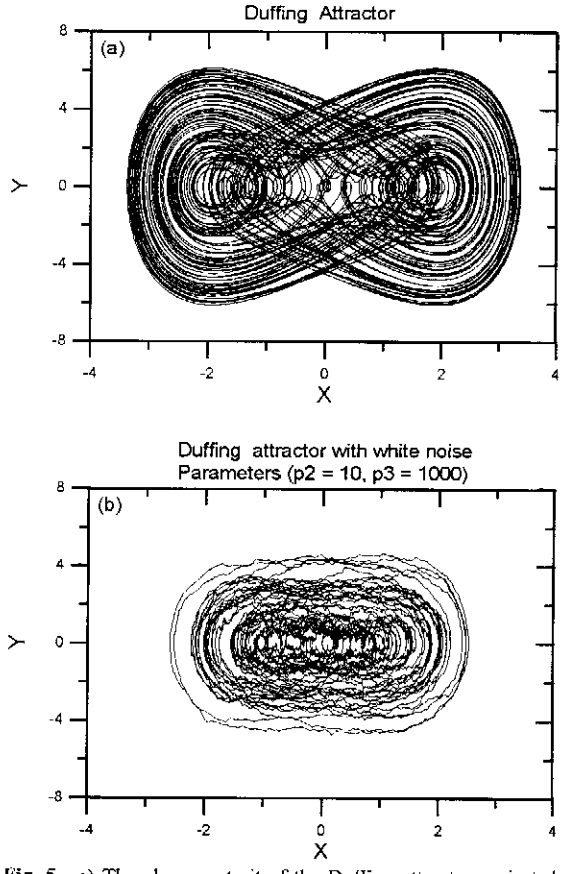

Fig. 5. a) The phase portrait of the Duffing attractor projected in the X-Y plane which corresponds to the solution of equation (6.5) for $k=0.05$ and $b=7.5$.

covered by the stochastic perturbation. More extensive study of the perturbed (input-output) limit point dynamics (node-focus, perturbed by white or colored noise) is going to be included in a separate study. Here we can declare that similar behavior has been found for different kinds of limit point dynamics and for different kinds of external stochastic perturbation. The above results support that the magnetospheric dynamics does not correspond to a stochastic limit point dynamics as the behavior of magnetospheric time series was found to be extremely different (Pavlos et al., 1999a; section *7* in this paper).

6.1.2 Stochastic torus

The next case is to suppose that the magnetospheric dynamics corresponds to the dynamics on a limit cycle or on a torus with external random perturbation. The results are similar for these two cases so that in the following we present only the case of a three dimensional torus. The dynamics on a n-dimensional torus can be described by a state vector $\boldsymbol{x}(t)$ given generally by the relation:

$$\boldsymbol{x}(t) = \sum_{n} c_n e^{i(\boldsymbol{n} \bullet \boldsymbol{w})t} \qquad (6.2)$$

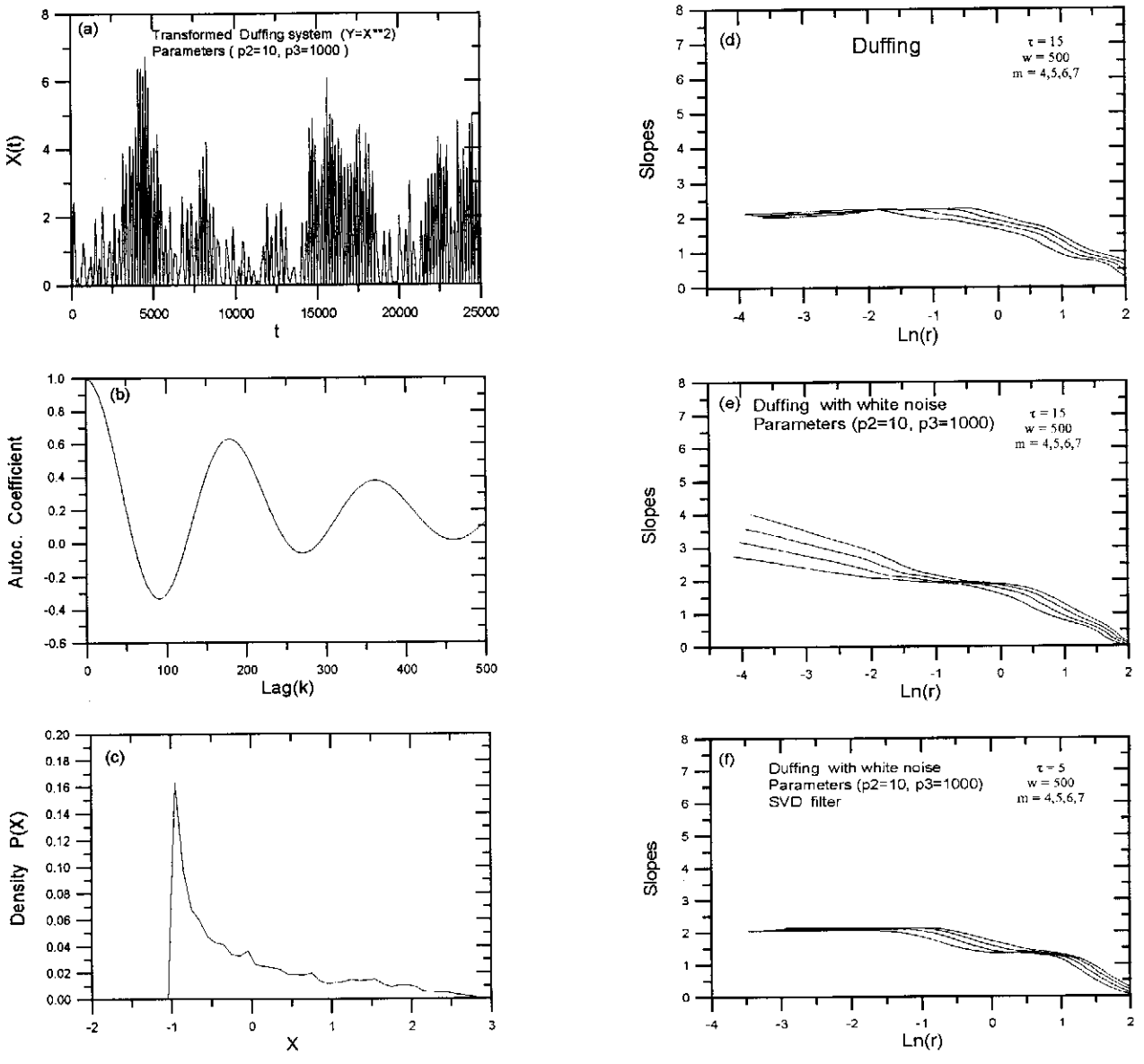

Fig. 6. a) The time series generated by stochastic equation of Duffing *(eq. 6.6)* for $p_2=10$, $p_3=1000$ and when a X^2 transform has been taken. b,c) Autocorrelation coefficient and amplitude distribution estimated for the time series shown in Fig. 6a. d) The slopes corresponding to the time series derived by the Duffing system without stochastic perturbation. e) Similar with *(d)* but for the time series of the stochastic system of Duffing. f) The same with *(e)* corresponding to the stochastic time series shown in *(d)* after an SVD filter was used.

where $\boldsymbol{n} \bullet \boldsymbol{w} = n_1w_1+n_2w_2+ \ldots +n_Nw_N$, and n_i integer. If the w_i are rational, only lines on the torus are covered. On the other hand the trajectory fills up the whole torus for irrational w_i. The dynamics on a torus can be caused either by a linear or non linear dynamics. In the following we use the signal of a 3-dimensional torus corresponding to the component:

$$x(t) = \sum_{n=1}^{3} c_n sinw_i t \qquad (6.3)$$

where $w_1=\sqrt{2}$, $w_2=\sqrt{3}$ *and* $w_3=\sqrt{5}$.

In order to make the signal to be as similar as possible with the magnetospheric signals (see paragraphs *7.1* and *7.2*) we take the X^2 transform of the above signal. The autocorrelation function of the above signal is periodic and the power spectrum discrete. In order the dynamics on the torus to mimic in a closer manner the magnetospheric dynamics, which reveals continuous power spectrum, we introduce a stochastic perturbation according to the relation:

$$x(t) = \sum_{n} (c_n + p_n w(t)) sinw_n t \qquad (6.4)$$

where p_n is the amplitude of the stochastic component and $w(t)$ is a white Gaussian noise with mean value zero and standard deviation one. Fig. 4a shows the square transformed signal of the stochastic 3-dimensional torus. Figs. 4(b-c) show the autocorrelation function and the amplitude distribution of the above signal. Fig. 4d includes the slopes of the correlation integrals estimated for the original (unperturbed) signal, while Fig. 4e is similar with Fig. 4d and corresponds to the stochastic torus signal shown in Fig. 4a. The correlation dimension of the unperturbed signal was found to a little higher than the value *3* which is the number of independent degrees of freedom of the dynamics on the 3-dimensional torus. This deviation from the value *3* may be caused by imperfection in the calculations. For the stochastic dynamics the slopes of the correlation integrals (shown in Fig. 4e) are perturbed at low values of the distance r in the reconstructed phase space, while they tend to conserve their plateau and saturation profile at high values of the r. As we ascertain in the following this is a general property of stochastic dynamical systems with low-dimensional internal dynamics. Fig. 4f is similar with Fig. 4e and corresponds to the SVD filtered signal of the stochastic torus dynamics. It is obvious from the figure that the SVD filter can remove the stochastic component, permitting the reappearance of the plateau profile and a low value saturation of the slopes. Although the correlation dimension is about one unit larger than the correlation dimension of the original deterministic signal the SVD filter is efficient to reveal the low-dimensional character of the stochastic signal. Moreover in order to exclude the case of low saturation caused by time related states in the embedding space we used the value $w=100$ for Theiler parameter. The above results show that the use of an SVD filter is efficient to reveal the low dimensional character of a stochastic signal which includes low dimensional deterministic component. As we show in section *7* the magnetospheric system reveals similar behavior with the stochastic low-dimensional torus concerning its correlation dimension estimated using an SVD filter.

6.1.3 Stochastic strange atractors

Nonlinear dynamical systems can bifurcate to strange attractor solutions after periodic solutions (limit cycle, limit torus). In order to study the influence of stochastic perturbation to the dynamics of strange attractors we use the system of Duffing defined by

$$\frac{d^2x}{dt^2} + k\frac{dx}{dt} + x^3 = bcost \qquad (6.5)$$

which describes forced damped nonlinear oscillations (Tsonis, 1992; Argyris et al., 1994). The external forcing is defined by the term $bcost$ and the dumping by the parameter k. As the magnetospheric system is a non-autonomous system perturbed randomly by the solar wind external coupling, a non-autonomous stochastic system of Duffing which behaves chaotically can be used as an appropriate model for studying the magnetospheric dynamics. The stochastic perturbation of the Duffing system is supposed to act at the amplitude and the frequency of the external driving force. This can be considered as an efficient imitation of the magnetospheric dynamo which also includes strong stochasticity caused by the solar wind as an input according to the previous analysis (see sections *3* and *4*). The stochastic Duffing system is described by:

$$\begin{aligned} \frac{dx_1}{dt} &= x_2 \\ \frac{dx_2}{dt} &= -kx_2 - x_1^3 + (b + p_1 w(t))cos(1 + p_2 w(t))x_3 \\ \frac{dx_3}{dt} &= 1 \end{aligned} \qquad (6.6)$$

Figs. 5(a-b) show the two-dimensional phase portrait of the original, purely deterministic strange attractor of the Duffing system and the stochastic strange attractor of Duffing system when a stochastic perturbation is included. It is apparent that while there is strong distortion of the trajectory, the system is not destroyed entirely. Figs. 6(a-c) present the time series corresponding to the square transformation of the x_2 variable, as well as its autocorrelation function and amplitude distribution. Fig. 6d shows the slopes of the correlation integrals estimated for the signal corresponding to purely deterministic component x_2 of the Duffing system. The slopes reveal that the correlation dimension of the strange attractor structure is $\cong 2.2$. Fig. 6e shows the slopes for the stochastic system of Duffing. This result is similar with theresult of a stochastic torus. That is, the plateau and the saturation profile of the slopes are destroyed gradually from low to high values of the distance r as we increase the stochastic coupling amplitude, and they remain invariable at high values of r for weak coupling. Fig. 6f presents the slopes of the system estimated for the stochastic time series after when an SVD filter was used. This figure shows that the use of an SVD filter can also remove the stochastic component of the above signal bringing the slopes to their original profile as it is seen by comparing Figs. 6f and 6d. Similar results have been observed for the x_2 squared signal described in Fig. 6e.

6.2 Deterministic input-output systems.

In this section we study the hypothesis that the magnetospheric system is a input-output system perturbed externally by a deterministic solar wind signal. As a prototype of this process we use the chaotic Duffing system

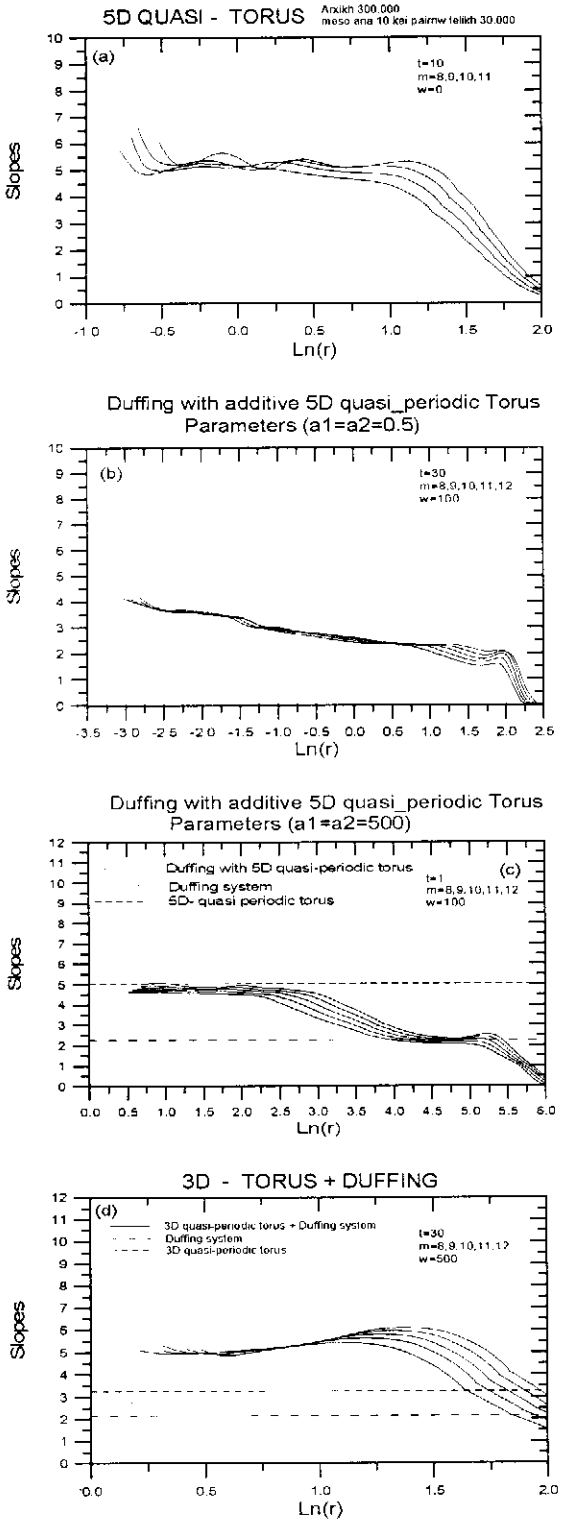

Fig. 7. The slopes of the correlation integrals for the time series corresponding to 5-dimensional quasi-periodic torus. b) Similar with *(a)* but for the time series corresponding to the Duffing system perturbed by the 5-dimensional quasi-periodic torus signal according to equations *(6.7)* for weak coupling with $a_1=a_2=0.5$. c) The same with *(b)* but for strong coupling with $a_1=a_2=500$. d) The slopes of the time series which was generated by simple addition of the signals corresponding to the Duffing system and the 3-dimensional quasi-periodic torus.

with input signal coming from a low dimensional deterministic dynamics. For our study we consider the case of the input signal generated by a deterministic dynamics on a 5-dimensional torus and the final input–output system is given by:

$$\frac{dx_1}{dt} = x_2 + a_1 y(t)$$

$$\frac{dx_2}{dt} = -kx_2 - x_1^3 + b\cos x_3 + a_2 y(t) \qquad (6.7)$$

$$\frac{dx_3}{dt} = 1$$

In this system $y(t)$ denotes the input generated the dynamics on a 5-dimensional torus and a_1, a_2 are the coupling amplitudes. Fig.7a shows the slopes corresponding to the signal of the 5-dimensional torus which is the input to the chaotic Duffing system. The plateau of the slopes and their saturation reveal the correlation dimension to be ~ 5 as it is expected. Figs. 7(b-c) show the slopes of the correlation integral estimated for the output of the perturbed Duffing system for weak and strong coupling with the external dynamics. In the first case of weak coupling we observe similar behavior with stochastic dynamical systems which include low-dimensional internal dynamics as the stochastic torus or the stochastic strange attractors (see Figs. 4e and 6e). That is, the plateau and the saturation profile of the slopes are destroyed at low value of r but they are conserved at high values. However while for stochastic systems the continuous increase of the coupling constant can finally destroy entirely the plateau and the saturation profile of the slopes, for deterministic input-output systems with low dimensional input the behavior is much different. That is for strong coupling amplitudes we can obtain the profile of the input system at low values of r while for high values of r the profile of the internal dynamics is conserved. This behavior is indicated by Fig. 7c where for small values of r there is a saturation of slopes similar with the corresponding profile of the input signal (see Fig. 7a) at value ~ 5. Moreover for large values of r the saturation value ~ 2.2 of the slopes is observed corresponding to the internal dynamics.

Similar behavior has been observed for additive input-output systems. In such systems we consider the input signal to be coupled additively with the output signal of the given dynamical system while no internal dynamical coupling exists. Such a kind of input-output dynamical system can be assumed appropriate for the magnetospheric system. According to the existed observations of the solar wind- magnetosphere interaction (see section *4*), the AE index time series reveals two additive components which correspond to different dynamical processes. The first is the driven deposition process and the second is the

loading–unloading process. In order to study such a composite process in the following we construct an additive signal composed by two dynamically independent signals. The first is derived by the deterministic dynamics on 3-dimensional torus and the second by the chaotic Duffing system described above. In this case the correlation dimension of the composite deterministic signal was found to be equal to the sum of the correlation dimensions corresponding to the original signals shown in Fig. 7d. As we can see in Fig. 7d the correlation dimension of the signal which was constructed to be the sum of a 3-dimensional torus signal and a ~ 2.2 dimensional strange attractor signal (Duffing signal) was estimated to be ~ 5.

6.3 Summary and conclusion for stochastic and deterministic input-output dynamical systems

Before we compare the above results with corresponding results from magnetospheric time series it is useful to summarize some crucial results concerning stochastic dynamics and input-output dynamics as they have been analyzed until now.

a) For experimental time series which reveal stationarity and broadband spectrum stochastic input-output dynamics is probably the most general model appropriate for the description of the underlying physical process. *In addition, when the slopes of the correlation integrals reveal efficient plateau and low value saturation profile for extended range of values of the radius r , then there is a low correlation dimension which is related to the deterministic internal component of the underlying process.* In this case the low correlation dimension indicates the existence of low dimensional internal determinism of the underlying physical process.

b) For non-autonomous systems the external stochastic or deterministic perturbation is not able to destroy entirely the profile of the internal dynamics. In both cases of stochastic (infinite dimensional) or deterministic (low dimensional) input the deterministic low dimensional profile of the slopes of the correlation integrals, estimated for output time series, is conserved at high values of the radius r in the reconstructed phase space, when the coupling amplitudes are not excessively large. In particular the external stochastic coupling destroys gradually the scaling of the correlation integrals and the saturation of their slopes as we increase the coupling constant and we go from low to high values of the radius r. Therefore when there exist noticeable plateau and saturation of the slope values only for large values of radius r and before the slopes begin to decrease, then this is strong evidence for a stochastic process with low-dimensional internal deterministic component. In the case of low dimensional deterministic input and strong coupling, the slopes reveal at low values of radius r the dimension of the input dynamics and at high values of radius r the dimension of the internal dynamics.

c) The saturation value of the slopes for a stochastic process is the same as the saturation value of the slopes corresponding to the purely deterministic component of the stochastic process. That is the noise which can be an infinite dimensional, or a high finite dimensional signal cannot increase considerably the saturation value of the slopes. It can only destroy the saturation profile when it is strong enough as the values of r gradually increase from small to large. Concerning an experimental time series, in which it is unavoidable the existence of a stochastic component, the above results are significant, because they show that the chaotic analysis can be used with confidence giving important information about the internal deterministic component of the observed signal.

d) In the case of time series derived by the dynamics of a stochastic limit point it is impossible to take low dimensional profile similar with the profile of a low-dimensional system. Given that the dimensionality of a limit point is zero we can conclude that the coupling of stochasticity and dynamics without rich internal structure in its phase space can not mimic low dimensional dynamics. Generally we can say that for the cases which were studied it is impossible for the stochasticity to create a fictitious low- dimensional profile of the slopes quite different from the low dimensional profile of the deterministic component of the underlying dynamics.

e) The use of an SVD filter can remove effectively the linear stochastic component of a signal with low dimensional deterministic component. Also the use of an SVD filter as a linear filter leaves invariant the dimensionality of the deterministic component of the original signal.

Finally all these results indicate that the modern nonlinear analysis of the experimental time series based on the embedding theory constitute a significant and useful tool for the detection of the characteristics of the underlying dynamical process. These conclusions make us to feel more confident about the results to be discussed in the following by studying magnetospheric signals.

7. Magnetospheric time series and magnetospheric dynamics.

In the studies by Pavlos et al. (1999a,b) it is shown that there is significant difference between the magnetospheric

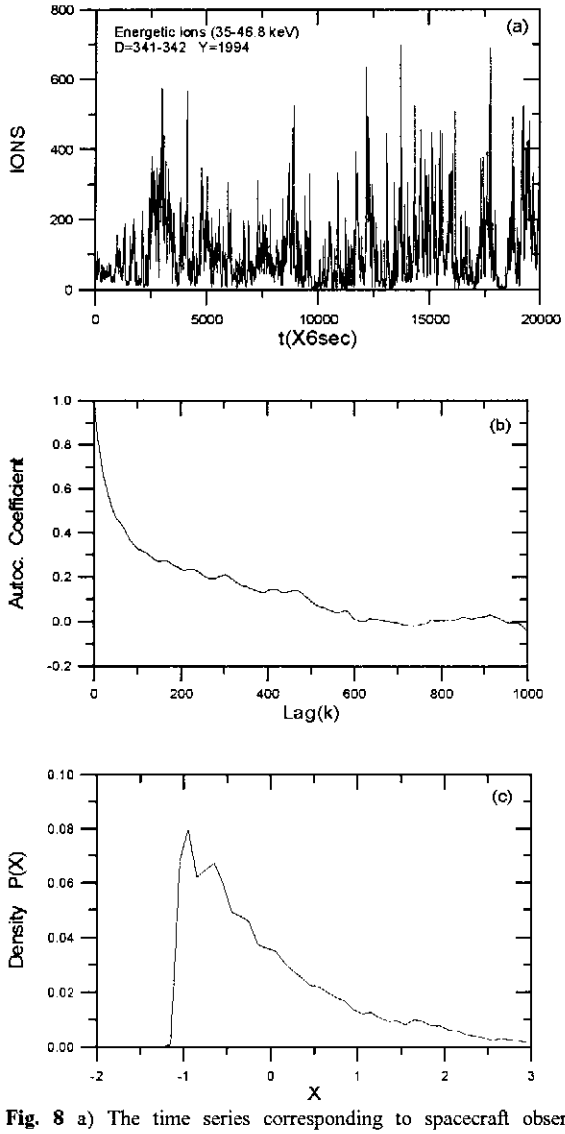

Fig. 8 a) The time series corresponding to spacecraft observations of energetic ions by the EPIC/ICS experiment. b,c) Autocorrelation coefficient and amplitude distribution estimated for the time series shown in *(a)*.

AE index and its surrogate data concerning the dynamical and geometrical characteristics of these time series. In this study we present some new results obtained by analyzing magnetospheric data which are associated with the results of the previous sections, especially those of sections *5* and *6* in order to decide about the magnetospheric dynamics.

7.1. Energetic ions time series

Fig. 8a shows measurements of magnetospheric energetic ions *(35-46.8 keV)* as they were observed by the experiment EPIC/ICS during the days *7-8* December of the year *1994* at the dawn magnetosheath of the earth's magnetosphere. This figure reveals strong and continuously repeatable bursts of energetic particles during *~30* hours. It is known that these particles are accelerated in the inner magnetosphere during periods with strong coupling of the magnetospheric system and the solar wind, simultaneously with strong bursts and enhancement of the AE index (Kirsch et al., 1984; Anagnostopoulos et al., 1986; 1998). It can be supposed that the dynamics of the energetic ions mirrors the internal magnetospheric dynamics similar with the AE index during periods with strong coupling of the magnetosphere and the solar wind (see Section *4*). The energetic particle differential fluxes are provided via the Energetic Particle and Ion Composition (EPIC) instrument of the GEOTAIL spacecraft essentially remained close to the ecliptic plane (Williams et al., 1994). The sampling time for the energetic ions analysed here was 6 sec.

The time series shown in Fig. 8a contains $N_T \cong 20.000$ data points. By using time series of magnetospheric energetic ions we avoid some obscurities included in the AE index that are going to be described in the next section concerning the discrimination between driven and loading-unloading process. Figs. 8b,c present the autocorrelation function and the amplitude distribution of the energetic ions time series. The first figure reveals abrupt decorrelation of the signal during the first *150 – 200* units of lag time which implies broadband spectrum. The second figure reveals that the distribution of the amplitudes is non-Gaussian which under certain conditions (especially when the signal is ergodic) indicates the possibility for the existence of nonlinearity in the signal. The nonlinearity can be dynamical or static something which will be clarified in the following by the method of surrogate data.

Fig. 9a shows the slopes of the correlation integrals estimated for the energetic ions time series and for embedding dimensions *m=4-7* without excluding time correlated states *(w=0)*. This figure reveals plateau and low value *($D \cong 3$)* saturation of the slopes. However this profile changes noticeably as we increase the value of Theiler parameter *w*. Fig. 9b is similar to Fig. 9a but for *w=50*. Now there is only a tendency for saturation at low values while the plateau is almost destroyed. The exclusion of time correlated states in the reconstructed phase space included in a sphere of radius *w* equal to the decorrelation time permits to discriminate between the self-affinity of the trajectory and the dynamical degrees of freedom. Therefore these results reveal the existence of strong component of noise in the observed time series which can destroy the scaling of the correlation integrals and the low value saturation profile of the slopes although some traces of these characteristics can survive. In order to remove the stochastic component we use an SVD filter described previously. Fig. 9c (solid lines) presents the slopes that were estimated for the SVD filtered energetic ions signal. Now we can notice that there is a clear scaling of the correlation integrals and a saturation of their slopes, at the value *$D \cong 2.5$*. The behavior of the energetic ions when an SVD filter is used is similar to the behavior of stochastic dynamical systems with low-dimensional internal determinism, (stochastic torus and strange attractor dynamics) as they were studied in section *6* (see Figs. (4e - f), and Figs. (6c-f). This similarity leads to the conclusion

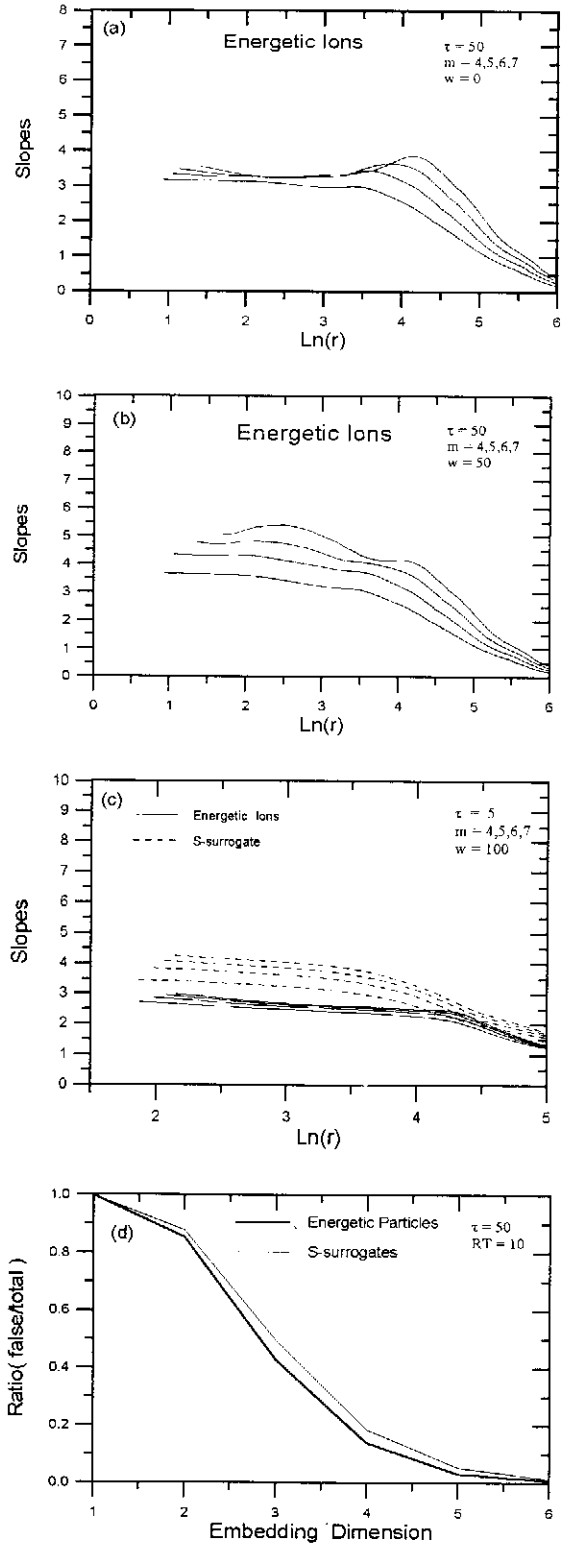

Fig. 9 a) Slopes of the correlation integrals as function of radius r for $m=4,5,6,7$, $\tau=50$ and $w=0$ corresponding to the time series shown in Fig. 8a. b) The same with *(a)* but for $w=50$. c) The same with *(a)* but for energetic ions and surrogate data time series after the application of an the SVD filter. d) The ratio of false to total nearest neighbors as function of the embedding dimension m estimated for the energetic ions signal and its surrogate for delay $\tau=50$ and parameter $R_T=10$.

of low-dimensional deterministic dynamics of the underlying process and to exclusion of a stochastic limit point dynamics. This process may be nonlinear as it was indicated by the profile of the amplitude distribution, and it is supported in the following by the method of surrogate data. The slopes of the correlation integrals estimated for the surrogate data of the energetic ions signal are presented in Fig. 9c. The surrogate data have been generated by the method of Schreiber and Schmitz (1996). As it is shown (Pavlos et al., 1999a,b), this method generates nonlinear stochastic data which can mimic faithfully the original time series (as far as the autocorrelation function and amplitude distribution is concerned), while they are derived by nonlinear static distortion of an original stochastic signal. It is apparent the significant difference between the slopes of the surrogate data and the original signal. The slopes of the surrogate data reveal values higher than the slopes of the original data while the plateau and the saturation profile are different. This result indicates that the deterministic component of the physical process underlyin the energetic ions signal physical process is nonlinear and low dimensional, excluding the possibility of static nonlinearity derived by a static distortion of an original linear stochastic signal. The low dimensional and dynamical non-linearity of the deterministic component of the underlying process is also supported by the estimation of false neighbors as a function of the embedding dimension m for the original signal and its surrogate data. The dynamical degrees of freedom of an experimental time series are equal to the minimum embedding dimension m of the reconstructed phase space for which the false crossing of the reconstructed trajectory and its false neighbors disappear (Abarbanel et al., 1993; Pavlos et al., 1999a). Fig. 9d shows the estimated values of the ratio of the false to total nearest neighbors as a function of the embedding dimension m for the original signal of the energetic ions (solid line) and its surrogate data (dashed line). The ratio false/total tends to zero for $m > 6$ which indicates that the independent degrees of freedom n of the underlying dynamical process can be equal to value $m=6$. In the same figure we can also observe the significant difference between the original and the surrogate data something which further supports the dynamic character of the non-linearity of the underlying process in the original time series of energetic ions. This result is in agreement with the estimated value of correlation dimension $D \cong 2.5$. According to embedding theory (see paragraph *5.2*), it is known that for correlation dimension D, it is efficient to describe the underlying dynamics by $n=2D+1$ independent degrees of freedom although it can happen n to be smaller. For our case this relation indicates $n \cong 6$ independent degrees of freedom. This is in accordance with the estimated value of the embedding dimension $m=6$ for which the false nearest neighbors are removed.

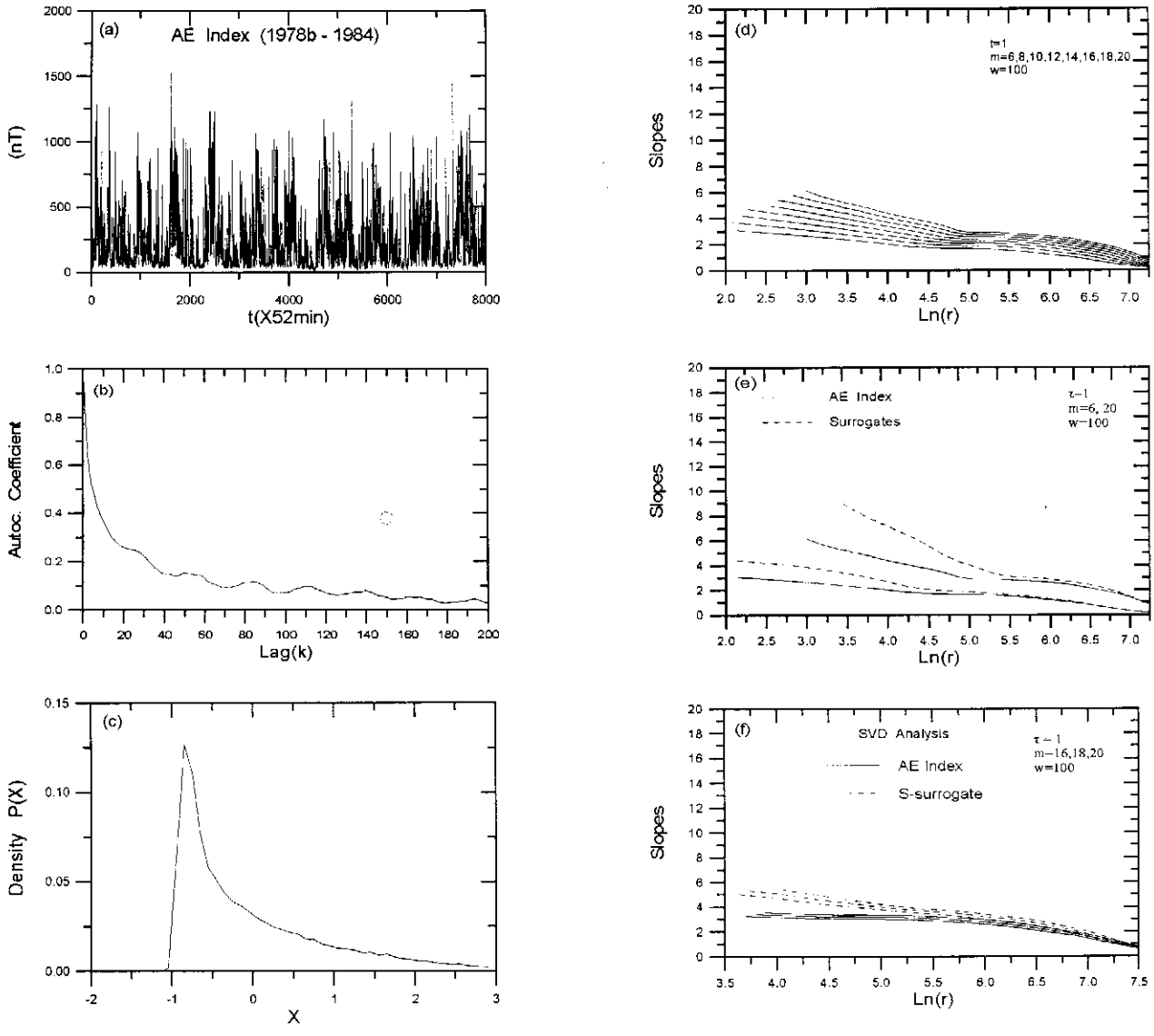

Fig. 10 a) The AE index time series during the period *1978b-1984* (*1978b* corresponds to the second semester of this year). b,c) Autocorrelation coefficient and amplitude distribution estimated for the signal shown in *(a)*. d) The slopes of the correlation integral estimated as function of r for m=*6-20*, w=*100* and τ=*1*. e) The same with *(d)* but for m=*6,20*, w=*10*, τ=*1*, corresponding to the AE index time series and its surrogate data. f) The same with *(e)* corresponding to the AE index after an SVD filter was used and its surrogate data.

7.2 The extended AE index time series

The AE index describes the Auroral-zone magnetic activity which is related with the global magnetospheric dynamics through a complex system of currents. The magnetospheric dynamics during substorms is manifested as strong variability of the magnetospheric and ionospheric electric currents especially the auroral electrojets (McPherron R.L., 1995). Disturbances in the Earth's magnetic field produced by currents in the magnetosphere and ionosphere are commonly described by a number of magnetic activity indices, which are derived from certain physical the disturbance. The indices AU, AL and AE give a measure of the strength of the auroral electrojets and are defined with the use of traces of the horizontal component (H) of the geomagnetic field measured by a world-wide chain of auroral-zone magnetic observatories (Davis and Sugiura, 1966). AU is the maximum positive disturbance (upper envelope) recorded by any station in the chain. AL is the minimum disturbance defined by the lower envelope of the traces of the chain. AE is defined by the separation of the envelopes (AE = AU-AL) in order to obtain a better measure of the strength of the auroral electrojets. The magnetospheric AE index time series has been used repeatively as a tool for the detection of the underlying magnetospheric dynamics and the testing of the hypothesis

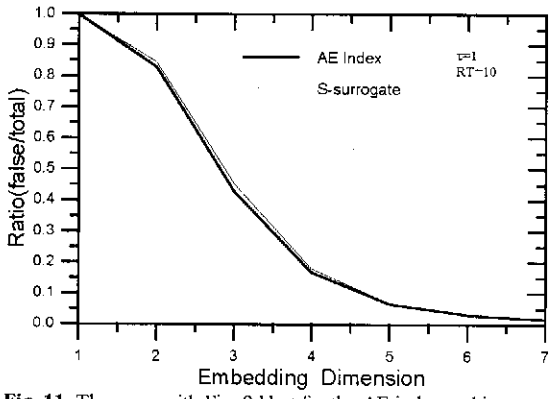

Fig. 11 The same with Fig. 9d but for the AE index and its surrogate.

of magnetospheric chaos (Vassiliadis et al., 1990; 1992; Shan et al., 1991; Roberts et al., 1991; Prichard and Price 1992, Pavlos et al., 1992a,b; Sharma et al., 1993; Takalo and Timonen, 1994; Pavlos et al., 1994). In the two studies (Pavlos et al., 1999a,b) we have used a long period of AE index during the second semester of the year *1978*, in contrast to previous studies in which much shorter periods of the AE index observation were used. In this paragraph we present results from the analysis of the much longer AE index observations. Fig. 10a presents the values of the AE index averaged per hour for the period *1978–1984,* while the sampling rate of the original signal was one minute. This time series has much longer length than the time series used in our previous work (Pavlos et al., 1992b; 1994, 1999a,b) as well as in the works of other scientists. Figs. 10(b-c) show the autocorrelation function and the amplitude distribution of the AE index. It is apparent the random character of the AE index with broadband spectrum as the autocorrelation coefficient shows an abrupt decay during the first ~ 200 minutes. The amplitude distribution (Fig. 10c) is non-Gaussian indicating possible nonlinearity (static or dynamic) similar to energetic ions. The slopes of the correlation integral estimated for this time series are shown in Fig. 10d for embedding $m=6\text{-}20$ and $w=100$. The profile of the slopes remains invariant for much larger values of w. In this figure we can see that the slopes of the AE index reveal similar profile with the slopes of low dimensional deterministic signals perturbed by a stochastic component. That is for low values of distance r there is no plateau or saturation of the slopes while these characteristics can be appeared at high values of r, ($\ln r \cong 5.00 - 6.00$), where there is a saturation value $D \cong 3.5$ of the slopes. This value is sensibly lower than the value $D \cong 5$ estimated in our previous study (Pavlos et al., 1999a) by using the AE index time series observed during a much smaller time period (only one semester). This difference can be understood to be caused by the long time period of the AE index that was used (*11* semesters), while the longer period implies better observation of the underlying dynamics. Fig. 10e shows a comparison of slopes for the original time series and its surrogate data. In this figure it is apparent the difference between the AE index and its surrogate data, especially at low values of r. Such a difference indicates the exclusion of the case of static non-linearity derived by a static distortion of an original linear stochastic signal. The exclusion of static non-linearity supports the hypothesis of dynamic non-linearity. An SVD filter also used for the case of the AE index. The result is included in Fig. 10f where the slopes of the filtered signal of the AE index and its filtered surrogate data are presented. For the AE index becomes obvious the removing of the stochastic component as the plateau and the saturation profile of the slopes appeared now at low values of r. The absence both of them (plateau and saturation) for the surrogate data after the SVD filtering confirms the dynamical non-linearity and the low-dimensionality for the process underlying the AE index. The final saturation value of the slopes is $D \cong 3.5$. The above results reveal that the behavior of the AE index when an SVD filter is used is similar with the stochastic and low dimensional dynamics of a torus and a strange attractor. That is the saturation value of the slopes *($D \cong 3.5$)* observed at large values of r before the use of an SVD filter is reappeared at small values of r after the application of the SVD filter. The ratio of false/total nearest neighbors estimated as function of embedding dimension for the AE index in its reconstructed phase space is shown in Fig. 11 (solid line), while the dashed line corresponds to the false/total nearest neighbors estimated for the surrogate data of the AE index. This ratio tends to zero for $m>7$, while for $m>5$ we observe coincidence of the ratios corresponding to the AE index and its surrogate data. The above results indicates at least $n \cong 7$ significant degrees of freedom and it is in accordance with the above value of the correlation dimension $D \cong 3.5$, which reveals that the degrees of freedom cannot be smaller than *4*. These results about the AE index time series are also in agreement with the results about the energetic ions time series. As these time series are observed at different regions of the magnetospheric systems the above coincidence it strengthens significantly the hypothesis of nonlinearity and low dimensionality of the magnetospheric system.

7.3 The SVD spectrum of the AE index.

According to the theoretical concepts included in paragraph *5.5*, the SVD analysis is appropriate to be used in order to obtain the deterministic components $v_i(t)$ of the AE index. In the estimation involved we have used observations only for the first six months of the above period *1978b-1984* described in Fig. 10a. Fig. 12a presents the first six months of AE index and its v_i autocorrelation function. Figs. 12(b-d) show only three ($i = 1,4,10$) time series of the ten corresponding to the SVD spectrum of the AE index. As we can see in this figure the amplitude of the values of the components are decreasing for increasing values of i. Figs 12(f-h) show the autocorrelation coefficient for the three v_i time series.

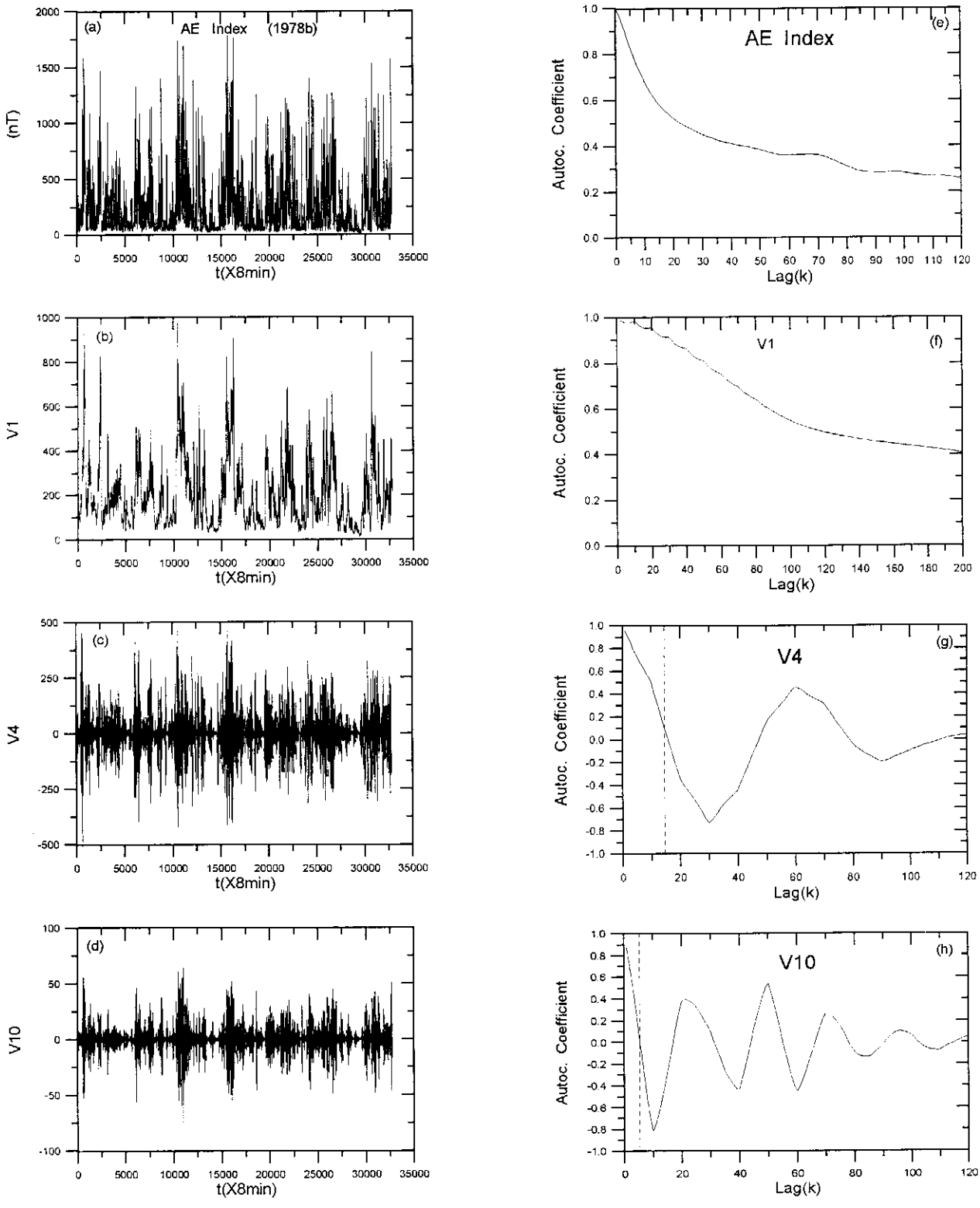

Fig. 12. a) The AE index time series corresponding to the second semester of the year 1978. b,c,d). The time series corresponding to the v_i, $i=1,4,10$, components of the SVD analysis of the signal shown in *(a)*. e,f,g,h) The autocorrelation coefficients estimated for the signals shown in *(a),(b),(c),(d)* respectively. The dotted lines indicate when the autocorrelation function in (g,h) become zero for first time.

The decorrelation times of the signals are decreasing for increasing values of i. According to SVD analysis every time series $v_i(t)$ corresponds to the projection of the trajectory on the eigenvectors e_i with eigenvalues σ_i respectively (see *(5.17)-(5.18)*). From the theoretical results of paragraph *5.5* the eigenvalues σ_i also decrease passing from low to high values of the index i so that the amplitude of the extension of the trajectory along the axis e_i

decreases as we go through from low to high values of the index i. Fig. 13a shows the spectrum of the singular values σ_i. In this figure it is clear that for $i > \sim 10$ the spectrum corresponds to the noise background. This indicates that approximately the deterministic components of the SVD spectrum are the first *10* components (v_i, $i=1-10$) and the nontrivial eigenvectors in the embedding space are the c_i, $i=1-10$. As the number of the nontrivial eigenvectors corresponds to the number of the degrees of freedom of the underlying dynamics we can conclude that the determinism of the underlying dynamics of the AE index shown in Fig. 12a includes ~ 10 independent degrees of freedom. This result can not be considered much different from the previous estimated number of ~ 7 degrees of freedom (see paragraphs *7.1* and *7.2*), since the AE index time series used here is only a small part of the time series presented in the estimations of the paragraph *7.2*.

The SVD spectrum (v_i) can be also used for the estimation of the dimension of the underlying process and for comparison with their surrogates data. In accordance with this, the slopes of the correlation dimension estimated for $(i < 8-10)$ reveal the characteristics of low dimensionality and non-linearity. Fig. 13b presents the slopes estimated for the component $v_4(t)$ and its surrogate data. Two things are clear, the low value saturation ($D \cong 3-4$) of the slopes and the significant difference with the slopes of the surrogate data. The same result was found for all the components except the first. As we can see in Fig. 13c the $v_1(t)$ component deviates from the above behavior, since the estimated slopes reveal that there is no saturation and no significant difference with the surrogate data. This anomaly can be interpreted as being caused by the existence of a component of the AE index which is externally driven by the direct coupling of the magnetosphere and solar wind and is only included in the first component of the SVD spectrum. In Fig. 12b it is seen that the $v_1(t)$ component corresponds mainly to the trend of the AE index time series shown in Fig. 12a and at the same time the $v_1(t)$ time series reveals long time decorrelation profile in comparison with the other components of the SVD spectrum. That is, the components v_i for $i > 1$ correspond to fast decorrelated processes (see Figs. 12(g-h), while the component v_1 is slowly decorrelated with decorrelation rate much slower than the original signal (see Figs. 12e-f). As the externally driven component corresponds to a smooth process (see Fig. 1 and descriptions in section *4*), it is reasonable to suppose that the driven component of the AE index is related mainly with the v_1 component. Therefore we conclude that SVD analysis can help to distinguish between the internal magnetospheric determinism related mainly with v_i $(i>1)$ and the external determinism which is mainly observed on the first component of the SVD spectrum. More details about this will be published elsewhere. We summarize now the results of time series analysis for the magnetospheric time series. In the studies (Pavlos et al., 1999a,b) we have

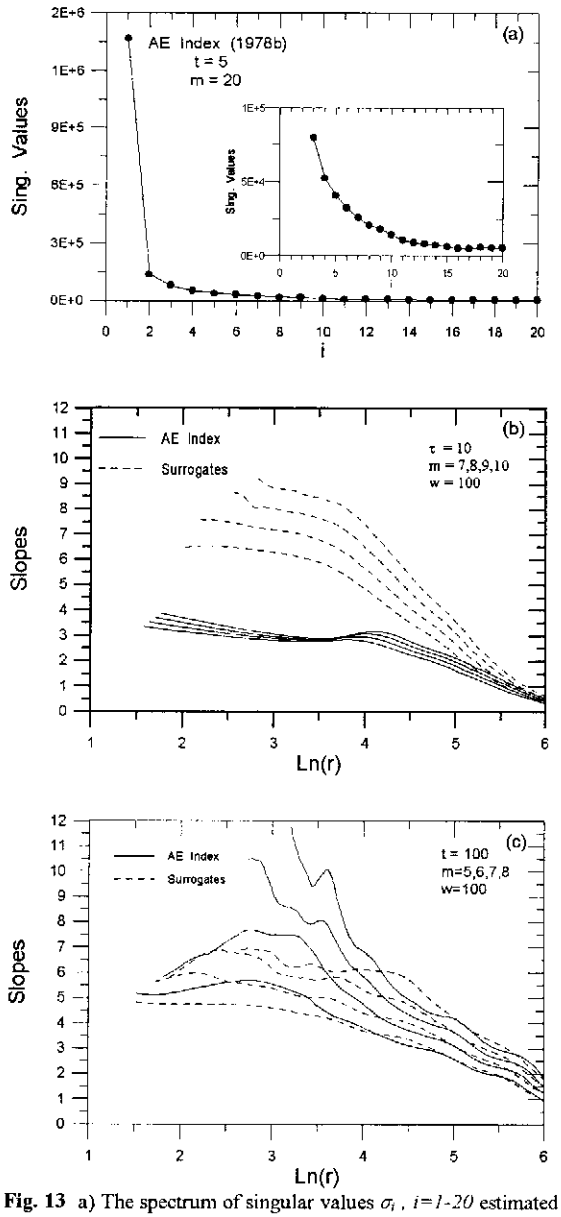

Fig. 13 a) The spectrum of singular values σ_i, $i=1-20$ estimated for the AE index time series shown in Fig. 12a. b) The slopes corresponding to the v_4 component of the SVD analysis of the AE index shown in Fig. 12a and the T-surrogate data of v_4. c) The same with (b) but for the v_1 component of the SVD analysis of the AE index.

shown significant difference between the AE index observed during the second semester of the year *1978* and its surrogate data. As discriminating statistics we had used geometrical and dynamical characteristics of the AE index. Here we have extended our analysis for two new time series concerning the estimation
of the underlying dynamics of the magnetospheric system. In the estimation of the dimension referred to dynamical characteristics of the time series we have used three independent methods: i) The slopes of the correlation integrals ii) the ratio false/total nearest neighbors and iii) the singular spectrum σ_i of the eigenvalues obtained by using SVD analysis. All these methods have given convergent results for the dimensionality of the supposed

magnetospheric attracting manifold at a low value $D \cong 3$-4. Moreover, we have found significant difference between the original time series and its surrogate data. These results are indicative for the magnetospheric dynamics and present an answer to a previous criticism, while the complete analysis of the magnetospheric energetic ions and the extended AE index will be published in a separate study.

8. Summary and conclusions

In this work we have included theoretical analysis and new experimental data in order to be able to acquire knowledge for understanding the magnetospheric dynamics. In section *2* we have reviewed the recent criticism against the hypothesis of magnetospheric chaos. One of the main objections was about the nonlinearity of the internal dynamics. That is, it is not possible to distinguish the magnetospheric AE index time series from surrogate data by using the correlation dimension as the discriminating statistic. The other objection was about the internal low dimensionality and chaoticity of the magnetospheric system. These characteristics (nonlinearity and low dimensionality) have been rejected because of the coupling between the magnetospheric system and the solar wind system. In addition a hypothesis was made that any non-linearity of the magnetospheric signal should be caused externally by the input signal, something which is expected as the magnetospheric system must be described as an input-output system according to recent studies (Price et al., 1994; Price and Prichard, 1993; Vassiliadis et al., 1992; Vassiliadis and Klimas, 1995; Pavlos et al; 1994). Therefore, in this and two other studies (Pavlos et al., 1999a,b) we have formulated the problem about the magnetospheric dynamics in the following way. At first we have asked if there is any separate internal magnetospheric dynamic. If something like this happens, then it must happen in combination with the external coupling of the magnetospheric system and the solar wind system. This makes the magnetosphere to be a complex input-output system. In this case it is more difficult to discriminate the internal dynamical characteristics from the coupling with the external dynamical characteristics. We believe that the theoretical and the experimental analysis included in this study and in two other studies (Pavlos et al., 1999a,b) can help significantly to elucidate these obscurities. In the following we summarize and discuss the crucial results of this study referred to the problem of the magnetospheric dynamics.

I) Theoretical concepts

The magnetospheric system can firstly be described as an non-linear infinite dimensional spatio-temporal system corresponding to a magnetized plasma system. In the section *3* we have supposed that the general theory of the order parameters and the slaving principle, which have been introduced for non-linear systems described by partial deferential equations, can also be applied to the magnetospheric system. In this theory the magnetospheric system is distinguished from other plasma systems by it own boundary conditions. The order parameters constitute the internal and the input dynamical magnitudes which could be identified with those magnitudes which are included in the macroscopic modeling of the magnetospheric dynamics (Baker et al., 1990; Pavlos et al., 1994) Although in this direction much work remains to be done, we can conclude that the theoretical description of the non-linear infinite dimensional magnetospheric plasma system may lead to a low dimensional macroscopic input-output description. According to this the macroscopic description of the magnetospheric system must include a low dimensional deterministic component $F(x, z)$ and a stochastic component $g(x, z, w)$ (see eq. *(3.7)* and *(3.8)*), with x describing the internal dynamics of the magnetospheric system, z the deterministic input dynamics of the solar wind and w a stochastic component. Both x and z constitute the order parameters of the magnetospheric system. Moreover the input $z(t)$ can be interpreted as a changing external control parameter, which makes the magnetospheric system to behave chaotically when it takes certain values. On the other hand the Wold's decomposition theorem of the classical time series analysis permits to separate a time series with continuous power spectrum to a purely linear deterministic component and to a purely stochastic component, while the whole process is a Markov process with both linear and nonlinear dynamical components. In the Wold's decomposition the linear deterministic component could be related with the external driving of the system while the random component could be related with the internal magnetospheric dynamics. This was found to be in agreement with the general profile of the AE index during substorm events (Fig. 1). The macroscopic stochastic component can be caused by an external or internal microscopic stochastic process. Moreover, according to time series theory, the magetospheric system can be assumed to behave as a recursive filter. This filter can be analyzed in a linear recursive component and a nonlinear recursive one. All the above theoretical descriptions could be possible models for the magnetospheric dynamics, which in general are input-output systems with a deterministic or stochastic input and a deterministic internal dynamics. Finally the SVD analysis, when examined from a theoretical point of view can be used in two ways. First as a filter and second to detect the deterministic dynamical component of the system. The above theoretical analysis has lead us to formulate the problem about the magnetospheric dynamics as follows:

a) Is there a macroscopic magnetospheric dynamics which

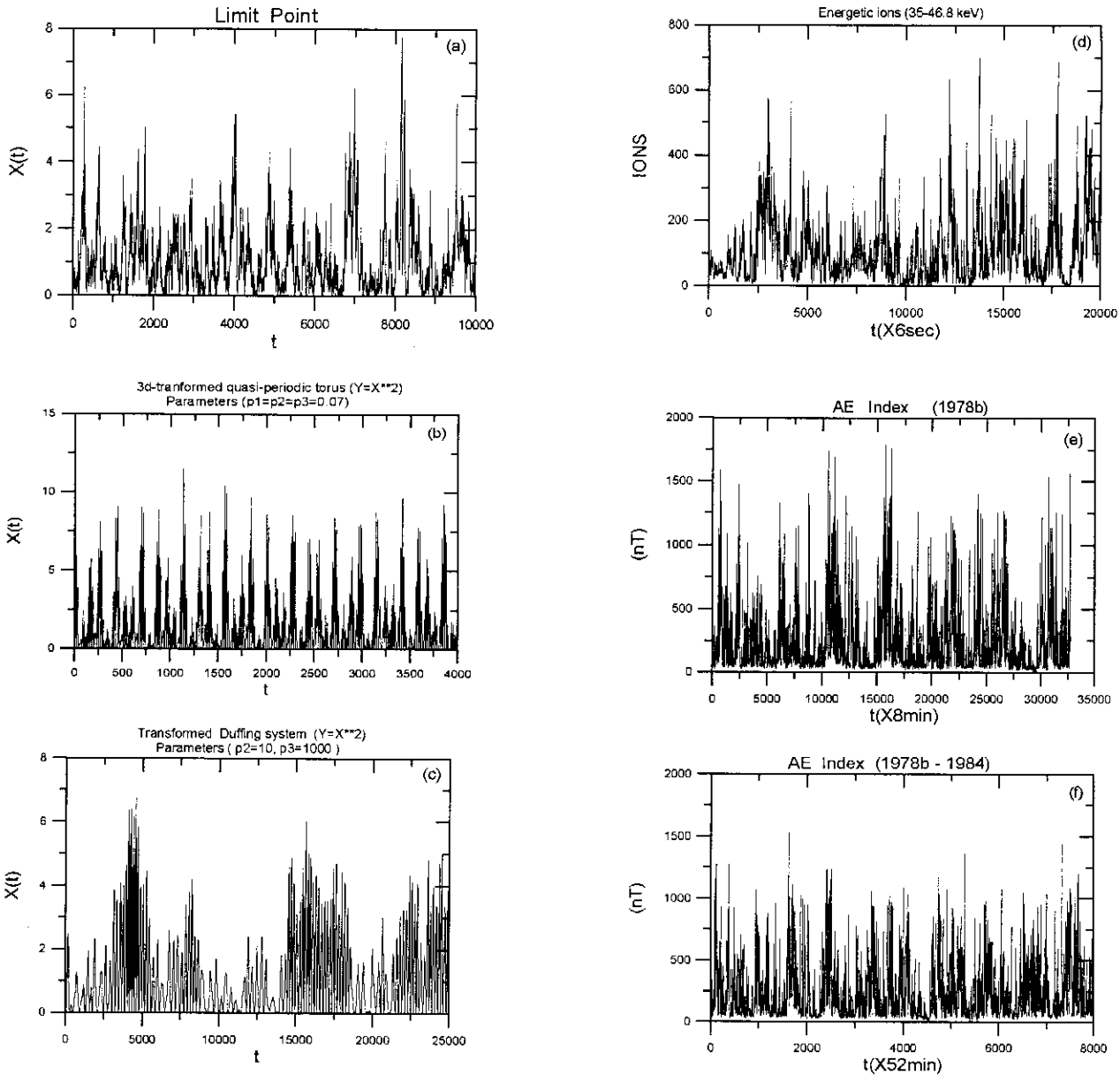

Fig. 14. This figure shows all the time series used in this study for comparison. It is noticeable the similarity of the different magnetospheric series and the stochastic systems, especially for the cases of the stochastic limit point and the stochastic quasi-periodic torus.

can be distinguished by the external solar wind dynamics?

b) If such a separate dynamics exists then is it low dimensional or high-dimensional, linear or non-linear and finally chaotic or non chaotic?

c) What is the relation between the internal magnetospheric dynamics and the external dynamics of the solar wind system

In order to answer these questions for the magnetospheric dynamics we have studied characteristic cases of stochastic systems and input-output dynamical systems which can be assumed to mimic the magnetospheric dynamics and some of its observed characteristics. Also we have estimated the correlation integrals, their slopes and the correlation dimensions of the time series derived by the above characteristic stochastic systems and input – output systems. The first system was related with a stochastic limit point dynamics. In this case we have shown that it is not possible for a stochastic system, with deterministic the second case we have used a non-autonomous system with external driving in order to obtain the greatest possible similarity with the magnetospheric system. It is shown that the stochastic perturbation cannot change dramatically the low dimensional profile of the deterministic component except when it is too strong, so that the stochasticity, becomes predominant and causes high dimensional profiles. The study of low-dimensional input-output dynamical systems has shown similar results, while the stochastic systems can be regarded as input-output systems with infinite dimensional input dynamics.

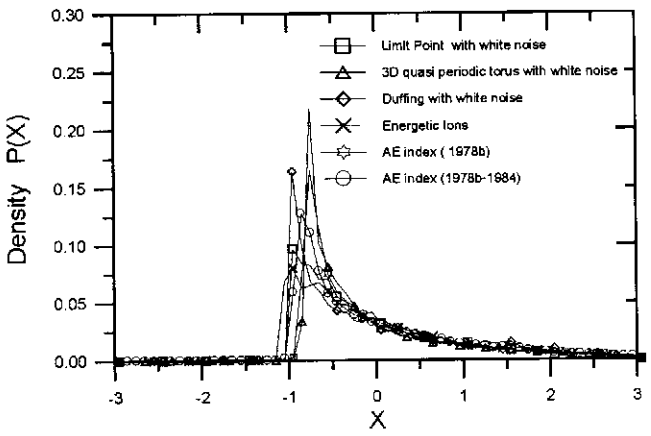

Fig. 15. The same with Fig. 14 but for the amplitude distributions.

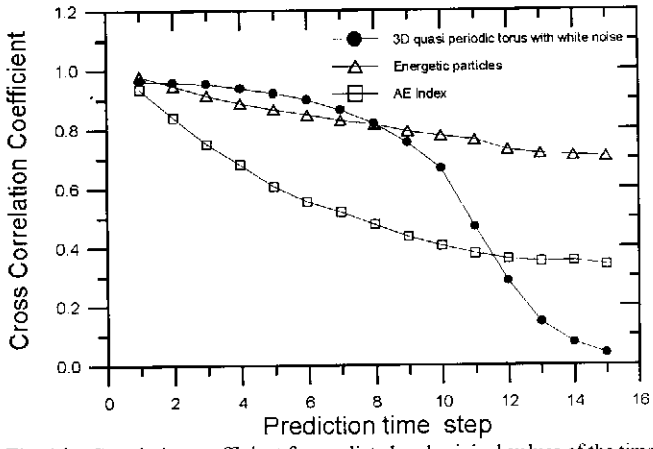

Fig. 16. Correlation coefficient for predicted and original values of the time series corresponding to the stochastic quasi-periodic torus signal and the two magnetospheric signals.

For this reason when we use as input to a dynamical system a low dimensional deterministic signal the results are analogous to the case of stochastic systems. That is, for weak input-output coupling the low-dimensional profile of the internal dynamics is conserved, while for strong coupling it is apparent the low-dimensional character for both the input signal and the internal dynamics. As a final case we studied input-output systems without an internal dynamics coupling where a simple additive system of two independent input dynamics is used. In this case the dimension of the output signal was found to be the sum of the dimensions of the original signals. *Therefore we have concluded that it is not possible to obtain low-dimensionality and chaotic profile by stochastic or input-output processes if such things do not exist in the internal dynamics of the system at least for the cases that have been analyzed until now.* As we have shown these results have been found to be crucial for understanding the magnetospheric system.

II) Experimental evidence

Moreover we have studied two new experimental magnetospheric time series. The first corresponds to energetic ions observed in situ by spacecraft at the outer magnetosphere and the second to an extended AE index time series observed during *13* semesters. The analysis of both time series has shown similar results although the time series correspond to much different magnetospheric magnitudes. The slopes of the correlation integrals estimated for these time series behave similarly as the slopes of the two stochastic systems, the stochastic torus and the stochastic strange attractor. That is, the plateau and the saturation profiles were observed only for high values of the distance r, while at low values of r the perturbation of noise was detected. For the AE index this behavior is quite clear. On the other hand the use of an SVD filter removed this anomaly at low distances r for both time series. That is, the plateau and the low-value saturation of the slopes which correspond to the filtered time series were observed to be present also at low values of distance r. Moreover these characteristics are absent for the surrogate data and remain invariable when we exclude enough number of time correlated points in the reconstructed phase space according to the test of Theiler. The low-dimensionality of the magnetospheric time series has also been supported by the method of false neighbors. Therefore these characteristics reveal similarity between the magnetospheric system and the stochastic systems with low-dimensional deterministic component. Figs. 14-15 show the profile of the magnetospheric time series and their statistical characteristics (amplitude distributions) in the comparison with time series derived by the stochastic systems described above. As these figures reveal there is noticeable similarity between time series derived from models and the experimental time series related to the magentospheric system. However the behavior of the above signals concerning their chaotic analysis is much different. The case of stochastic limit point is excluded as a candidate for the magnetospheric dynamics as its slopes do not reveal low-dimensional profile. The case of the stochastic torus can also be excluded by comparing the behavior of its time series and the magnetospheric time series from the point of view of prediction algorithms. Fig. 16 presents the cross-correlation of the predicted and the original values for the magnetospheric and the stochastic torus time series. For this method we have used local linear prediction methods (Pavlos et al., 1999b). In this figure we observe that the predictability for energetic particle time series is better than the AE index times series, while in both cases is a smooth decrease of the cross-correlation coefficients when the prediction time step increases. On the other hand for the first ten steps ahead the predictability of the stochastic torus time series, which is by construction a linear signal, is almost the same with that of the energetic particles but much better than the predictability of the AE index. For prediction time larger than *12* steps ahead the predictability of the stochastic torus signal decreases abruptly to values close to zero,

while the energetic particles show best predictability. Therefore, we conclude that a) the energetic particle time series include stronger determinism than the AE index signal b)the long term predictability of the magnetospheric signals compared with the stochastic torus indicate low-dimensional chaotic dynamics.

Finally we believe that the arguments discussed above help us exclude the stochastic limit point and stochastic torus as candidate models of the magnetopsheric system leaving the stochastic strange attractor dyanamics as the only possible model of the magnetospheric system. We believe that the results of this comparison study will not alter significantly even if the above-studied low dimensional stochastic systems can mimic much better the magnetospheric time series. Moreover the Duffing system is significant for the above conclusions as it is non-autonomous and externally driven, similar with the magnetosphere. That is, the stochastic perturbation of the amplitude and the frequency of the external driving of the Duffing system can simulate satisfactorily the random character of the solar wind driving on the magnetospheric system.

Furthermore description of the low-dimensional input-output modeling has been indicated for the magnetospheric system. We have already indicated that input-output systems are distinguished from stochastic systems from the point of the view of the dimensionality of the input signal. For stochastic systems the input signal is infinite dimensional while for low dimensional input-output systems the input is a deterministic finite dimensional signal. In this work we have studied two different kinds of input-output systems in comparison with the magnetospheric system. The first input-output system includes a rich low-dimensional dynamics corresponding to the Duffing system with input a deterministic 5-dimensional signal. The second input-output system is much simpler and corresponds to the addition of two low-dimensional deterministic signals. The first can simulate the magnetospheric system only in the case that the coupling is weak, which makes the input-output model to be equivalent to a stochastic model. For strong coupling the first kind of input-output system can clearly reveal the low-dimensional character of the input signal at low values of distance r in the reconstructed phase space. However such a character is absent in the profile of the slopes of the magnetospheric time series. In the second case of the additive input-output modeling dynamics we must suppose that the saturation value $D \cong 2\text{-}3$ of the slopes estimated for the magnetospheric signals must be the sum of the dimension of the internal and the dimension of the external signal. This could be true only if the correlation dimensions of the solar wind input signal and the dimension of the magnetospheric signals are much lower than the above estimated value $D \cong 2\text{-}3$. However such a supposition cannot be true as the solar wind signals do not reveal correlation dimension lower than the magnetospheric dimensions (Pavlos et al., 1992a,b). Finally excluding the low-dimensional input-output modeling, we can suppose that the magnetospheric system behaves as a recursive filter for the solar wind input signal. It is shown that linear and non-recursive filtering leaves invariant the correlation dimension of the input signal (Broomhead at al., 1992). For recursive linear or nonlinear filtering it is possible to observe change in the correlation dimension as we move from the input to output signal. However the existence of recursive character in the filter is equivalent to the existence of internal dynamics separate from the dynamics of the input signal. In this case the recursive filter corresponds to a input-output system with rich internal dynamics which can be mirrored at the correlation dimension of the output signal, in accordance with the above results for input-output systems. Also the non-linear and non-recursive filtering can cause change in the correlation dimension of the input signal but this case corresponds to static nonlinear distortion and can be excluded by the method of surrogate data. Furthermore, for the magnetospheric system it has been indicated that there is small evidence for the presence of non-linear deterministic coupling between the solar wind input and the magnetospheric output (Price et al., 1994). As the solar wind time series reveal much higher correlation dimension than the magnetospheric time series (Pavlos et al., 1992a,b) we can suppose that the internal magnetospheric process is the main cause of the low correlation dimension for the magnetospheric time series.

Another interesting point is that the SVD spectrum of the AE index for one semester observations has shown low value of independent degrees of freedom $(n \cong 10)$. The $v_i(t)$ components $(i<10)$ reveal significant low dimensional determinism much different than the corresponding surrogate data, except for the first component $v_1(t)$. The $v_1(t)$ component describes the projection of the trajectory on the eigenvector c_1 which corresponds to the larger value of determinism. We have interpreted this anomaly as being caused by that component of AE index which is externally driven although this supposition must be worked further in a forcoming paper. These results support further the existence of low-dimensional magnetospheric internal dynamics. Finally we conclude that the random character of the magnetospheric time series could be caused by the chaotic low-dimensional internal dynamics of the magnetospheric system, while this character only appears when the solar wind input takes appropriate values. As the solar wind is changing continuously its state, the magnetospheric dynamics can live intermittently on a low-dimensional chaotic attractor. However we believe that, although we have revised in a noticeable degree of confidence the hypothesis of magnetospheric chaos, much work remains to be done in different directions before we accept certainly this point of view.

Acknowledgements. We would like to thank three anonymous referees for their valuable comments which led to the improvement in the quality of the paper.

References

Abarbanel, H. D., Brown, R., Sidorowich, J. J., Tsirming, L. S., The analysis of observed chaotic data in physical systems, *Rev. Mod. Phys., 65*, 1331-1392, 1993.

Akasofu, S.-I., Energy coupling between the solar wind and the magnetosphere, *Space Sci. Rev., 28*, 121-190, 1981.

Anagnostopoulos, G. C., Sarris, E. T., and Krimigis, S. M., Magnetospheric origin of energetic (E≥50 keV) ions upstream of the bow shock: The October 31, 1977, event, *J. Geophys. Res. 91*, 3020-3028, 1986.

Anagnostopoulos, G. C., Rigas, A. G., Sarris, E. T., and Krimigis, S. M., Characteristics of upstream energetic (E≥50 keV) ion events during intense geomagnetic activity, *J. Geophys. Res., 103*, 9521-9533, 1998.

Argyris, J., Faust, G., Haase, M., An exploration of chaos, 1994, Elsevier , Amsterdam, 1994.

Argyris, J., Andreadis, I., Pavlos, G., Athanasiou, M., On the influence of noise on the Largest Lyapunov exponent and on the geometric structure of attractors, *Chaos, Solitons & Fractals, 9*, 947-958, 1998.

Baker, D. N., Klimas, A. J., McPherron, R. L., and Bucher, J., The evolution from weak to strong geomagnetic activity: an interpretation in terms of deterministic chaos, *Geophys. Res. Lett., 17*, 41-44, 1990.

Baker, D. N., Klimas, A. J., Vassiliadis, D. V., Energy transfer between the solar wind and the magnetosphere-ionosphere system, *J. Geomagnetism and geoelectricity 47*, 1171-1182, 1995

Bhattacharjee, J. K., Convection and chaos in fluids, World Scientific, Singapore, 1987.

Brogan, W. L., Modern control theory, Prentice Hall, Englewood Cliffs, New Jersey, 1982.

Broomhead, D. S. and King, G. P., Extracting qualitive dynamics from experimental data, *Physica D, 20*, 217-236, 1986.

Broomhead, D. S.,. Huke, J. P., and Muldoon, M. R., Linear filters and non-linear systems, *J.R. Statist. Soc. B*, 1992.

Casdagli, M., Jardin, D. D., Eubank, S., Farmer, J. D., Gibson, J., Hunter N., and Theiler, J. Non linear modeling of chaotic time series: Theory and applications, in Applied Chaos, editors H. Kim and J. Stringer, pp 335 – 380, John Wiley & Sons, New York 1992.

Chua, L. O., Yong, Y., and Yang, Q., Generating randomness from chaos and constructing chaos with randomness, *Int. J. Circ. Theor. App., 18*, 215-240, 1990.

Cook, P. A., Nonlinear dynamical systems, Prentice Hall International, London, Limited 1994.

Davis, T. N. and Sugiura, M., Auroral electrojet activity index AE and its universal time variation, *J. Geophys. Res., 71* (3), 785-801, 1966.

Farmer, D. J., and Sidorowich, J. J., Predicting chaotic time series, *Phys. Rev. Lett., 59*, 845-848, 1987.

Gapanov-Grekhov A. V. and Rabinovich, M. I., Nonlinearities in action, Springer- Verlag, Berlin Heidelberg, 1992.

Grassberger, P. and Procaccia, I., Measuring the strangeness of strange attractors, *Phys. D, 9*, 189-208, 1983.

Haken, H., Advanced synergetics, Springer, Berlin Heidelberg, 1983.

Haken, H., Information and self-organization, Springer, Berlin, 1988.

Hao Bai-Lin, Chaos, World Scientific, Signapore 1984.

Hones, E.W., Transient phenomena in the magnetotail and their relation to substorms, *Space Sci. Rev., 23*, 393-410, 1979.

Kan, J. R., Synthesizing a global model of substorms, Magnetospheric substorms, American Geophysical-Union,1991.

Kirsch, E., Pavlos, G. P., and Sarris, E. T. ,Evidence for particle acceleration processes in the magnetotail, *J. Geophys. Res., 89*, 1003-1007, 1984.

Klimas, A. J., Baker, D. N., Roberts, D. A., Fairfield, D. H., and Buchner, J. A., A Nonlinear dynamic model of substorms, *Geophys. Monog. Ser., vol. 64*, edited by J.R. Kan, T.A. Potemra, S. Kokumun, and Iijima, pp. 449-459. AGU. Washington, D.C., 1991.

Klimas, A. J., Baker, D. N., Roberts, D. A., and Fairfield, D. H., A nonlinear dynamical analogue model of geomagnetic activity, *J. Geophys. Res., 97*, 12253-12266, 1992.

Klimas, A. J., Vassiliadis, D., Baker, D. N., and Roberts, D. A., The organized nonlinear dynamics of the magnetosphere, *J. Geophys. Res., 101*, 13089-13113, 1996.

Klimas, A. J., Vassiliadis, D., Baker, D. N., Data-derived analogues of the magnetospheric dynamics, *J. Geophys. Res.,102*, 26993-27009,1997.

Lee, L. C., Fu, Z. F., and Akasofu, S. I., A simulation study of forced reconnection process and magnetospheric storms and substorms, J. *Geophys. Res., 90*, 10896, 1985.

Liu, Z. X., Lee, L. C., Wei, C. Q., and Akasofu, S., I. Magnetospheric substorms: an equivalent circuit approach, *J. Geophys. Res., 93*, 7355-7366, 1988.

Lorenz, E. N., Deterministic nonperiodic Flow, J. Atmos. Sci., 20, 130, 1963.

McPherron, R. L., Magnetospheric substorms, *Rev. Geophys. Space Phys., 17*, 657-681, 1979.

McPherron, R. L., Magnetospheric dynamics, Introduction to space physics, edited by M.G. Kivelson, C.T. Russell, 400-458, Cambridge University Press, 1995.

Osborne, A. R., Kirwan, A. D., Provenzale A., and Bergamasco, L., A search for chaotic behavior in large and mesoscale motions in the Pacific Ocean, *Physica D, 23*, 75-83,1986.

Osborne, A. R. and Provenzale, A., Finite correlation dimension for stochastic systems with power-low spectra, *Physica D, 35*, 357-381, 1989.

Papadopoulos, K., The role of microturbulence on collisionless reconnection, in Dynamics of the magnetosphere, edited by S. I. Akasofu, pp. 289-307. D. Reidel, Dordrecht, 1980.

Pavlos, G. P., Magnetospheric dynamics, in Proc. Symposium on Solar and Space Physics, edited by D. Dialetis, pp. 1-43. National Observatory of Athens, Athens 1988.

Pavlos, G. P., Rigas, A. G., Dialetis, D., Sarris, E. T., Karakatsanis, L. P., and Tsonis, A. A., Evidence for chaotic dynamics in outer solar plasma and the earth magnetopause, in Chaotic Dynamics: Theory and Practice, edited by A. Bountis, pp. 327-339. Plenum, New York, 1992a.

Pavlos, G. P., Kyriakou, G. A., Rigas, A. G., Liatsis, P. I., Trochoutos, P. C., and Tsonis, A. A., Evidence for strange attractor structures in space plasmas, *Ann. Geophys., 10*, 309-322, 1992b.

Pavlos, G. P., Diamadidis, D., Adamopoulos, A., Rigas, A. G., Daglis. I. A., and Sarris, E. T., Chaos and magnetospheric dynamics, *Nonlin. Proc. Geophys., 1*. 124-135, 1994

Pavlos, G. P., Athanasiu, M., Kugiumtzis, D., Hantzigeorgiu, N., Rigas A. G., and Sarris, E. T., Nonlinear analysis of Magnetospheric data , Part I. Geometric characteristics of the AE index time series and comparison with nonlinear surrogate data. (accepted for publication in *Nonlin. Proc. Geophys.*, 1999a).

Pavlos, G. P., Kugiumtzis, D., Athanasiu M., Hantzigeorgiu, N., Diamantidis D., and Sarris, E. T., Nonlinear analysis of Magnetospheric data , Part II. Dynamical characteristics of the AE index time series and comparison with nonlinear surrogate data. (accepted for publication in *Nonlin. Proc. Geophys.*, 1999b).

Prichard, D. J., and Price, C. P., Spurious dimensions estimates from time series of geomegnetic indices, *Geophys. Res. Lett., 19*, 1623-1626, 1992.

Price, C. P. and Prichard, D., The non-linear response of the magnetosphere: 30 October 1978, *Geophys. Res. Lett., 20*, 771-774, 1993.

Price, C. P., Prichard, D., and Bischoff, J. E., Nonlinear input/output analysis of the auroral electrojet index, *J.Geophys. Res., 99*, 13227-13238, 1994.

Prichard, D. J., and Price, C. P., Is the AE Index re result of nonlinear dynamics? *Geophys. Res. Lett., 20*, 2817-2820, 1993.

Prichard, D. J., Short comment for magnmetospheric chaos, *Nonlinear Proc. Geophys, 20*,771-774, 1995.

Prigogine, I. and Nicolis, G., Self-organization in nonequilibrium systems: towards a dynamics of complexity, Bifurcation Analysis, edited by M. Hazewinkel, R. Jurkovich and J. H. P. Paelinck, pp.3–12, published by D. Reidel, Dordrecht, 1985.

Priestley, M. B., Non-linear and non-stationary time series analysis, Academic Press, London, 1988.

Provenzale, A., Osborne, A. R., Kirwan, Jr. A. D., and Bergamasco, L., The study of fluid parcel trajectories in large-scale ocean flows, in Nonlinear Topics in Ocean Physics, edited by A.R. Osborne, pp. 367-402, Elsevier, Paris, 1991.

Provenzale, A., Smith, L. A., Vio, R., and Murante, G., Distinguishing low dimensional dynamics and randomness in measured time series, *Physica D, 58*,31-49, 1992.

Roberts, D. A., Baker, D. N., Klimas A. J., and Bargatze, L. F., Indications of low dimensionality in magnetospheric dynamics, *Geophys. Res. Lett., 18*, 151-154, 1991.

Rostoker, G., Observational constraints for substorm models, American Geophysical Union, 1991.

Shan, H., Hansen, P., Goertz, C. K., and Smith, K. A., Chaotic appearance of the AE Index, *Geophys. Res. Lett., 18,* 147-150, 1991.

Sarma, A. S., Vassiliadis D., and Papadopoulos, K., Reconstruction of low-dimensional dynamics by singular spectrum analysis, *Geophys. Res. Lett., 20,* 335-338, 1993

Shaw, R. Z., The dripping faucet as a model dynamical system, Aerial Press, Santa Cruz, CA, 1984.

Schreiber, T. and Schmitz A., Improved surrogate data for nonlinearity test, *Phys. Rev. Lett., 77,* 635-638, 1996.

Spiegel, E. A. and Weiss, N. O., Magnetic activity and variations in solar luminosity, *Nature 287,* 616-617, 1980.

Spiegel, E. A., Cosmic arrithmias, J.R. Buchler et al., (eds), Chaos in Astrophysics, 91-135, D. Reidel publishing company, 1985.

Summers, D. and Mu., J. L., On the existence of a Lorenz strange attractor in magnetospheric convection dynamics, *Geophys. Res. Lett., 19,* 1899-1902, 1992.

Takalo, J. and Timonen, J., Properties of AE data and bicolored noise, J. *Geophys. Res., 99,* 13239-13249, 1994.

Takens, F., Detecting strange attractors in turbulence, in Vol. 898 of Lectures Notes in Mathematics, edited by D.A. Rand and L.S. Young, pp. 366-381. Spinger, Berlin, 1981.

Takens, F., On the numerical determination of the dimension of an attractor, in dynamical systems and bifurcations, Groningen 1984, in vol. 1125 of Lecture Notes in Mathematics, pp. 99-106, edited by B.L.J. Braakama, H.W. Broer, and F. Takens, Berlin, Springer-Verlag, 1985.

Teman, R., Infinite – dimensional dynamical systems in mechanics and physics, Springer-Verlag, New York, 1988.

Theiler, J., Some comments on the correlations dimensions of $1/f^{a}$ noise, *Phys. Lett. A, 155,* 480-493, 1991.

Theiler, J., Galdikian, B., Longtin, A., Eubank, S., and Farmer, J.D., Using surrogate data to detect nonlinearity in time series, in Nonlinear Modeling and Forecasting, vol. XII of SFI studies in the Sciences of Complexity, edited by M. Casdagli and S. Eubank, p. 163-188, Addison-Wesley, Reading, Mass., 1992a.

Theiler, J., Eubank, S., Longtin, A., Galdikian, B., and Farmer, J. D., Testing for nonlinearity in time series: the method of surrogate data, *Physica D, 58,* 77-94, 1992b.

Theiler, J., Linsay, P. S., and Rubin, D. M., Detecting nonlinearity in data with long coherence times, Time series prediction, forecasting the future and understanding the past, Vol. XV of SFI studies in the Sciences of Complexity, edited by A.S. Weigend and N.A. Gershenfeld, Addison-Wesley, 1993.

Tong, H., Non-linear time series, a dynamical system approach, Oxford University Press, New York, 1990.

Tsonis, A. A., Chaos: From theory to applications, Plenum Press, New York, 1992.

Weigend, A. S. and Gershenfeld, N. A., Time Series Prediction: Forecasting the Future and Understanding the Past. Addison-Wesley Publishing Company, Reading, 1994.

Weiss, N. O., Kattaneo, F., and Jones, C. A., Periodic and aperiodic dynamo waves, *Geophys. Astrphys. Fluid Dynamics, 30,* 305-341, 1984.

Weiss, N.O., Periodicity and aperiodicity in solar activity, Phil. Trans. R. Soc. Lond. A, 330, 617 – 625, 1990.

Williams, D. J., McEntire, R. W., Schemm, C., II, Lui, A.T.Y., Gloeckler, G., Christon, S.P., and Gliem, F., GEOTAIL energetic particles and ion composition instrument, *J. Geomagn. Geoelectr., 46,* 39-57, 1994.

Vassiliadis, D., Sharma, A. S., Eastman, T. E., and Papadopoulos, K., Low-Dimensional chaos in magnetospheric activity from AE time series, Geophys. *Res. Lett. 17,* 1841-1844, 1990.

Vassiliadis, D., Sharma, A. S., and Papadopoulos, K., Time series analysis of magnetospheric activity using nonlinear dynamical methods, in Chaotic Dynamics: Theory and Practice, edited by T. Bountis, Plenum, New York, 1992.

Vassiliadis, D. and Daglis, I. A., A diagnostic for input-output nonlinear systems: The effect of a nonlinear filter on the correlation dimension, MPAE-W-100-93-32 report, 1993.

Vassiliadis, D. and Klimas, A. J., On the uniqueness of linear moving-average filters for the solar wind-auroral geomagnetic activity coupling, J. *Geophys. Res. 100,* 5637-5641, 1995.